Parametric Finite Element Analysis for a square cup deep drawing process

F. Ayari [a], E. Bayraktar [b],*

[a] Laboratory of Mechanics, College of Science and Technology,
1008 Montfleury, Tunis, Tunisia
[b] Supmeca/LISMMA-Paris, School of Mechanical
and Manufacturing Engineering, Paris, France
* Corresponding author: E-mail address: bayraktar@supmeca.fr

Analysis and modelling

ABSTRACT

Purpose: This manuscript deals with the FEA of the sheet metal forming process that involves various nonlinearities. Our objective is to develop a parametric study that can leads mainly to predict accurately the final geometry of the sheet blank and the distribution of strains and stresses and also to control various forming defects, such as thinning as well as parameters affecting strongly the final form of the sheet after forming process.

Design/methodology/approach: The main approach of the current paper is to conduct a validation study of the FEM model. In fact, a 3D parametric FEA model is build using Abaqus /Explicit standard code. Numerous available test data was compared to theoretical predictions via our model. Here, several elastic plastic materials low was used in the FEA model and then, they were validated via experimental results.

Findings: Several 2D and 3D plots, which can be used to predict incipient thinning strengths for sheets with flat initial configuration, have been presented for the various loading conditions. Unfortunately, most professionals in the forming process, lack this expertise, which is an obstacle to fully exploit the potential of optimization process of metal forming structures. In this study optimization approach is used to improve the final quality of a deep drawn product d by determining the optimal values of geometric tools parameters.

Research limitations/implications: This paper is a first part study of a numerical parametric investigation that is dealing with the most influent parameters in a forming process to simulate the deep drawing of square cup (such as geometric, material parameters and coefficient of frictions). In the future it will be possible to get a large amount of information about typical sheet forming process with various material and geometric parameters and to control them in order to get the most accurate final form under particular loading, material and geometric cases.

Originality/value: This model is used with conjunction with optimisation tool to classify geometric parameters that are participating to failure criterion. A mono objective function has been developed within this study to optimise this forming process as a very practical user friend manual.

Keywords: FEM; Deep drawing; Plasticity; Friction; Explicit method; Parametric study; Modelling; Optimization; Clusters

Reference to this paper should be given in the following way:

F. Ayari, E. Bayraktar, Parametric Finite Element Analysis for a square cup deep drawing process, Journal of Achievements in Materials and Manufacturing Engineering 48/1 (2011) 64-86.

1. Introduction

In this study we are analysing the forming of three dimensional shapes by deep drawing process. Different numerical process can be used as it is mentioned in the literature [1-5].

The most efficient way to analyse this type of problem is to analyse the forming step with a FEM code that allows both dynamic and static analysis. In this study, Abaqus Explicit [6] is used to carry FE analysis. Since the forming process is essentially a quasi-static problem, computations with Abaqus /Explicit are performed over a sufficiently long time period to render inertial effects negligible.

Forming processes are generally expensive, for this reason there is a great amount of researches studies related to their optimizations. Indeed, the coupling of simulation software's with mathematical algorithms for optimizing the process parameters is widely increasing in various fields of forming. It was demonstrated that this kind of coupling reduces and improves the products' cost [7].

Optimization of process parameters such as die radius, blank holder force, friction coefficient, etc., can be accomplished based on their degree of importance on the sheet metal forming characteristics. In this investigation, a statistical approach based on computing with categorical array technique was adopted to determine the degree of importance of some geometric design parameters on the thickness distribution of deep drawn rectangular cup. Then a mono objective optimization method scheme has been applied in forming study to design the process providing guidance how to choose the best fixed geometric parameter which leads to the selected minimum failure criterion.

2. Description of the initial model

The material of the blank will form the base of the cup which is in contact with the face of the punch, the die and the holder. This material can stretch and slides over the surface of the punch; however, minimal variation in thickness of this material is expected (Figure 1).

During a deep drawing operation, the blank is subjected to radial stresses due to the blank being pulled into the die cavity and there is also a compressive stress normal to the element which is due to the blank-holder pressure. Radial tensile stresses lead to compressive hoop stresses because of the reduction in the circumferential direction.

In fact, the load applied on the blank is modelled as a distributed load on the contact surface holder-blank. The wall of the cup is primarily encountering a longitudinal tensile stress, as the punch transmits the drawing force through walls of the cup and through the holder as it is drawn into the die cavity. There is also a tensile hoop stress caused by the cup being held tightly over the punch.

The choice of the different geometric dimensions and material properties was conformed to experimental previous data. In fact, before starting the parametric FE study, we have performed a comparative study with experimental previous work and we have used it as a validation study of this model. All the initial dimensions are chosen to be identical to those used in the experimental previous study [7]. The blank is initially square, 150 mm by 150 mm, and is 0.78 mm for the (mild steel Ms, that

is the material chosen to be studied in this work). The rigid die is a flat surface with a square hole 84 mm by 84 mm, rounded at the edges with a radius of 8 mm. The rigid punch measures 70 mm by 70 mm and is rounded at the edges with the same 10 mm radius. The blank holder can be considered a flat plate, since the blank never comes close to its edges. The geometry of these parts is illustrated by Figure 1 and Figure 2. The rigid surfaces are offset from the blank by half the thickness of the blank to account for the shell thickness.

a)

b)
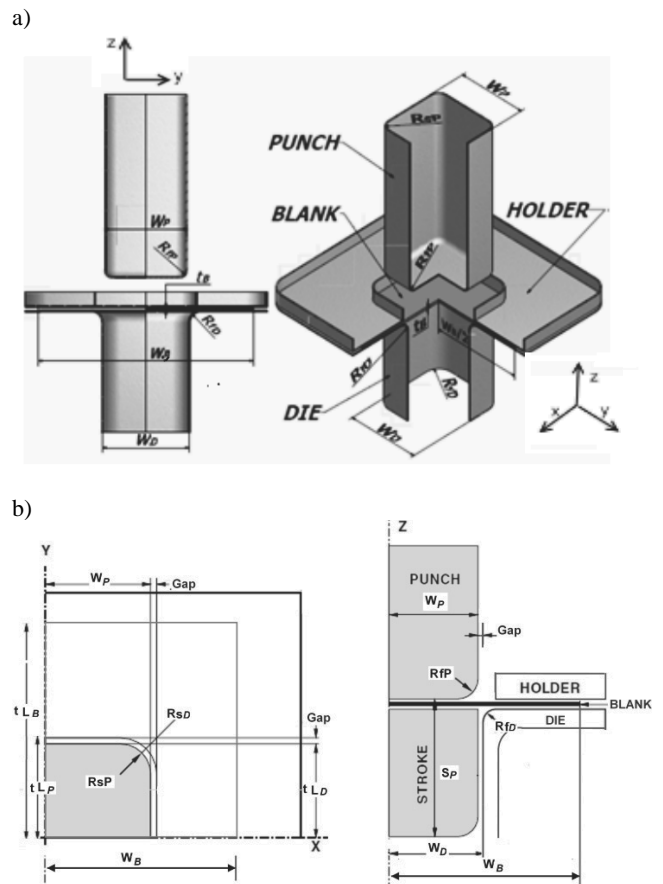
Fig. 1. a) 3D key dimensions of the FE assembly model; b) principal geometric parameters of the FE model

While Abaqus/Explicit automatically takes the shell thickness into account during the contact calculation. A mass of 0.65 kg is attached to the blank holder, and a concentrated load of 19.6 kN is applied to the contact surface blank - holder. The blank holder is then allowed to move only in the vertical direction to accommodate changes in the blank thickness. The coefficient of friction between the sheet and the punch is taken to be variable from (0.01 to 0.125), and that between the Blank and the Punch. It is (from 0.01 to 0.25). In fact, in previous studies it was confirmed that the coefficient of friction between contact surfaces has an important effect in the forming process [1].

The simulated punch velocity is kept constant and equal to 1.66 mm/sec while the considered minimum nodal distance is less than the blank thickness.

a)

b)
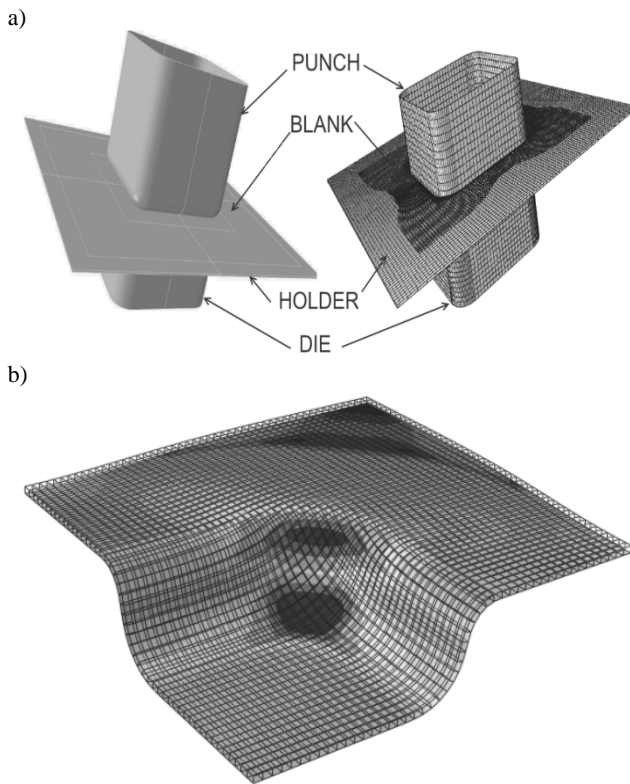
Fig. 2. a) FEA model of the DDP of a square cup; b) FEA model of the DDP of a square cup; blank mesh

The blank is made of Mild steel Ms. The relation between true stress and logarithmic strain, stress strain of this materials are done with the following expressions [7].

$$\sigma = 565.32 \left(0.007117 + \bar{\varepsilon}^P\right)^{0.2589} \ \text{MPa} \qquad (1)$$

where σ is the equivalent tensile stress, ε^P the equivalent plastic strain and the other material parameters are identified by mechanical tests (Table 1). Figure 3 shows the equivalent stress vs. the plastic deformation of the MS with different test directions.

Table 1.
Material properties

	Mild Steel
σ_Y *(Mpa)*	173.1
E (GPa)	206
σ_{US} *(MPa)*	311.4
ρ *(kg/m³)*	7800

The stress-strain behaviour is defined by piecewise linear segments matching the Ramberg-Osgood curve up to a total (logarithmic) strain level of 107%, with Mises yield, isotropic hardening, and no rate dependence.

Given the symmetry of the problem, it is sufficient to model only a one-quarter sector of the box. However, we have employed a one-quarter model to make it easier to visualize. We use 4-node, three-dimensional rigid surface elements (type R_3D_4) to model the die, the punch, and the blank holder. The blank is modelled with 8-node, linear finite-strain shell elements (type SC8R).
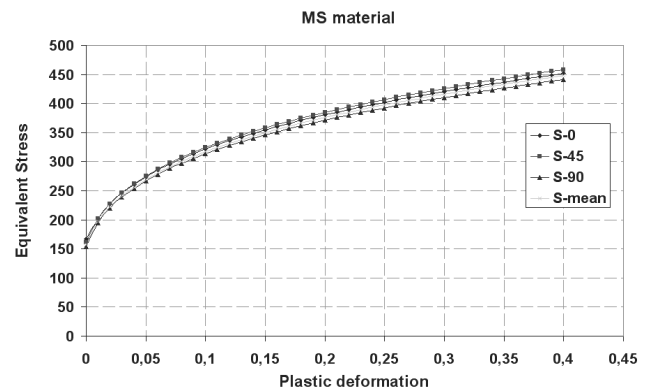
Fig. 3. The stress-strain curve used for the numerical simulations

The computer time involved in running the simulation using explicit time integration with a given mesh is directly proportional to the time period of the event, since the stable time increment size is a function of the mesh size (length) and the material stiffness. Thus, it is usually desirable to run the simulation at an artificially high speed compared to the physical process. If the speed in the simulation is increased too much, the solution does not correspond to the low-speed physical problem; i.e., inertial effects begin to dominate. In a typical forming process the punch may move at speeds on the order of 1 m/sec, which is extremely slow compared to typical wave speeds in the materials to be formed. (The wave speed in steel is approximately 5000 m/sec.) In general, inertia forces will not play a dominant role for forming rates that are considerably higher than the nominal 1 m/sec rates found in the physical problem.

In the results presented here, the drawing process is simulated by moving the reference node for the punch downward through a total distance of 11- 15- 30 and 40 mm (6.626506, 9.036145, 18.072289 and 24.096386). In this analysis we used the technique of mass scaling to adjust the effective punch velocity without altering the material properties.

3. The FEM model

Finite element simulations of deep drawing process provide an effective means to investigate the interaction between the process parameters and the material response. They provide useful information for fine-tuning the production processes. In this study the deep drawing process of rectangular cups is modelled using FEA. The general purpose commercial FEA code Abaqus/Explicit is used for the simulations.

The movement of the punch was defined using a pilot node. This node was also employed to obtain the drawing force during the simulation. After applying appropriate boundary conditions to the models of sheet, punch, die and blank holder, the numerical simulation of the process was performed.

Figure 4 shows the simulation with 51 elements. The distribution of the von Mises stresses is illustrated in Figure 4a for the numerical analysis with 106 solid elements. To facilitate doing a comparison between various results, the remaining of the FE findings are presented and discussed in the next section.

a)   b)

c)
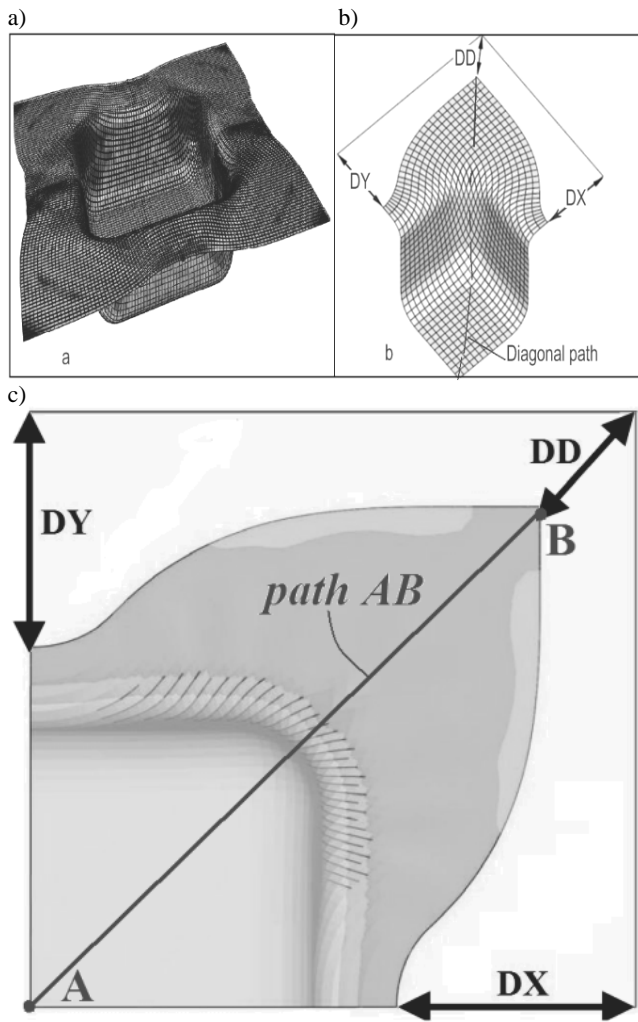
Fig. 4. a) Earing profile of the blank at the end of the DDP; b) direction used for FE validation study; c) X-Y plane projection of the DD, DX and DY earing profile measurements distances and AB Strain sampling path

4. Validation study

To check the validity of results computed by deep drawing simulations, two numerical comparative studies were investigated. Results from these two studies were compared to experimental results and a good correlation was deduced. These parameters refer to mild steel sheets.

4.1. First validation with general displacements

The first validation study consists on a comparison between numerical and experimental displacements in the following directions: DX-called 'rolling direction', DD (diagonal direction) and DY (transverse direction) as shown in Figure 4.

Table 2 below illustrates results obtained for a square blank with a punch stroke of 15 mm and 40 mm for Mild steel material. Earring profile shows asymmetric flow. In fact, in deep drawing it derives from planar anisotropy. Thus, the plastic flow of anisotropic sheet can be regarded as the sum of two superimposed deformation processes occurring simultaneously; normal flow controlled by normal anisotropy, and asymmetric flow due to planar anisotropy. In fact, before the parametric study, a blank sheet mesh size sensitivity study has been built and as it is shown by the Figure 5 above a mesh size of 55, the earring profiles dimensions DX, DY and DD are insensitive to the mesh size variation. That is the reason for which we have adopted the 55 mesh size as the optimal value in the model.

Table 2.
Comparative results of experimental study

Material	*Ms*	*Ms*
Travel	15 mm	40 mm
DX_FEA	7.07	28.6
DX_EXP	7.0	28.1
DX_ERROR	**1.0%**	**1.8%**
DD_FEA	3.7	14.89
DD_EXP	3.9	15.1
DD_ERROR	**5.1%**	**1.4%**
DY_FEA	7.06	28.6
DY_EXP	7.1	28.5
DY_ERROR	**0.6%**	**0.4%**
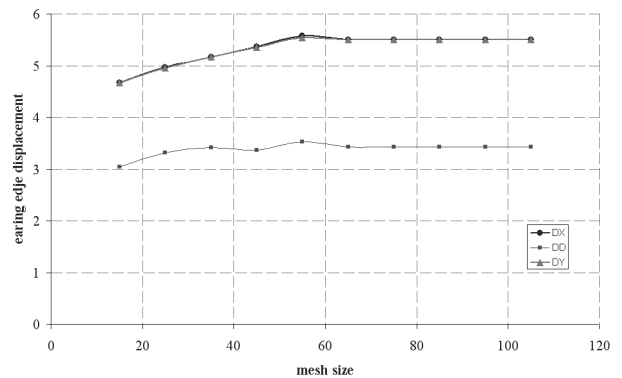
Fig. 5. Curve that demonstrates the mesh sensitivity

The numerical results presented in the Table 1 are obtained with the following coefficient of friction 0.02 for the Blank Holder contact, 0.02 for the Blank Die contact, 0.25 for the Punch Blank contact and then 0.034 for the Blank Holder contact, 0.04 for the Blank for the global contact surfaces for MS material and 0.0 Die contact, 0.16 for the Punch Blank contact, then 0.04 for the global contact surfaces for the Al material. These coefficients are chosen to simulate the real contact surfaces of the experimental conditions; as before each experiment both sides of the Blank sheet surface were wiped with a paper towel dipped in the lubricant and they were kept in a vertical position for 30 minutes [7]. Thus, we have conducted several finite element simulations by varying the Blank- Holder coefficient of friction, the Blank Die coefficient of friction and the Blank Punch coefficient of friction in the range from 0 to 0.25. We have measured at each time the edge displacements which are describing the earring

profile in the X direction, the Y direction and the Diagonal direction. These displacements values were then compared to those obtained experimentally for the Ms Material. Results from Table 1 show that experimental and FE earring profile displacements were being close so that the error is varying from 1% to 5.1%.

4.2. Strain comparative study

The second validation to be considered in this study, consists of the comparison between the experimental and the numerical principle strains (ε_1, ε_2, ε_3) in the diagonal direction of the blank denoted by the path AB (Figure 4), for a punch travel of respectively 15 mm and 40 mm with the MS material (Figs. 6, 7).

The experimental strain profiles trend, along the diagonal path, was closely replicated by the FEA model. In particular, Figure 7d. shows a slight gap in the plot between thickness strain and distance along diagonal displacement of the Mild steel with 40 mm travel punch. The difference between experimental and numerical strains in this case is due to an important out of plan strain deformation for x = 75 mm (at the vicinity of the corner cup for which a maximum thinning is denoted). In general, the numerical values overestimate the biaxial state flow strain. As far as we are dealing with high anisotropic materials, the Von Mises criterion used for numerical strains predictions overestimates the experimental strain values, but this discrepancy can be allowed as the maximum error between numerical and experimental thickness strains does not exceed the 18% except for the MS with

ultimate punch stroke of 40 mm. Yet, the simulation results produced the trend in deformation behaviour of the MS blank. In all the cases, the elements in the corner area do not reach a state of plastic instability even within a draw depth of 40 mm.

5. Parametric FEM study

Finite element simulations of deep drawing process provide an effective means to investigate the interaction between the process parameters and the material response. They provide useful information for fine-tuning the production processes. In this study the deep drawing process of rectangular cups is modelled using FEA. The general purpose commercial FEA code Abaqus/Explicit 6.7 is used for the simulations.

5.1. Model geometry

All parts are modelled as rigid bodies except for the blank which is modelled as an elastic-plastic material with metal plasticity. The DDP simulation is accomplished in two phases: the blank holder applies a predetermined force on the blank then a displacement equal to the desired depth is applied to the punch.

All geometric dimensions of the parts may vary and the model geometry can be easily changed. Parts used in the DDP are shown by Figure 1b, principal dimensions of a cup shown therein may be
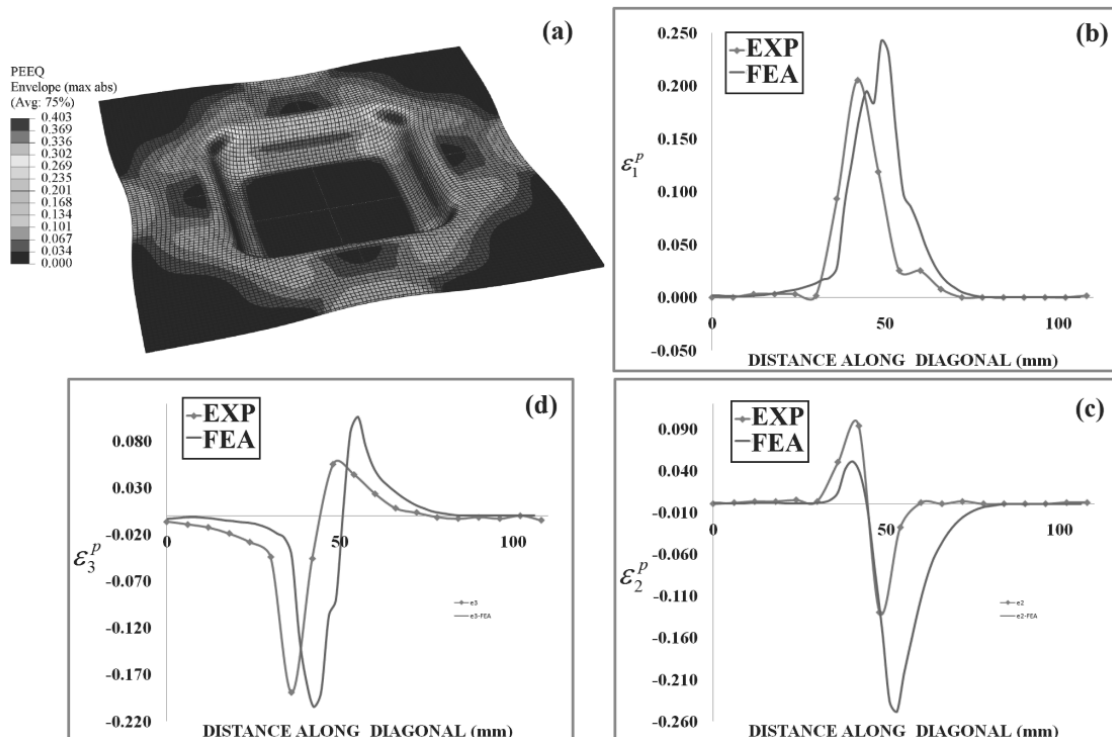
Fig. 6. Comparison between FEA and experimental results for Mild steel with punch travel of 15 mm: a) Mises stress distribution and deformed shape of the square cup; b) Principal strain ε_1 along diagonal path AB; c) Principal strain ε_2 along diagonal path AB; d) Principal strain ε_3 along diagonal path AB
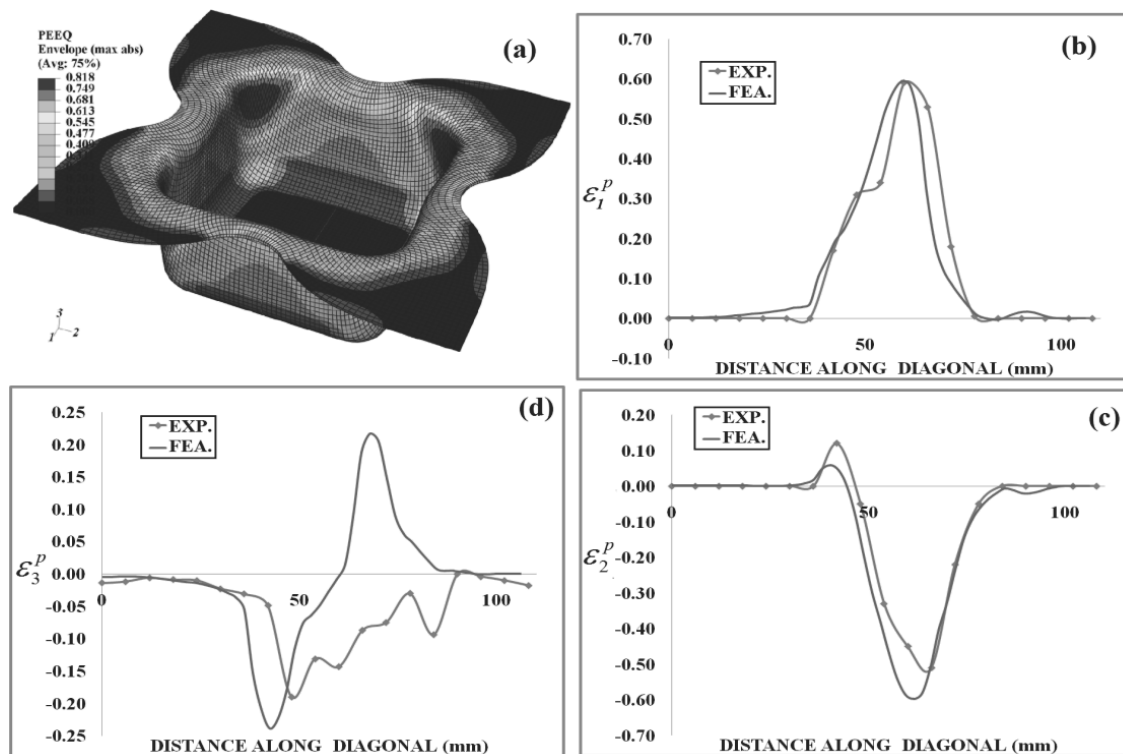
Fig. 7. Comparison between FEA and experimental results for Mild steel with punch travel of 40 mm: a) Mises stress distribution and deformed shape of the square cup; b) Principal strain ε_1 along diagonal path AB; c) Principal strain ε_2 along diagonal path AB; d) Principal strain ε_3 along diagonal path AB

varied in the FE model. Thus, the Figure 1b describes the geometric parameters of the deep cup model. In fact, t_b is the blank thickness, W_P is the punch width section, W_B is the blank width section, W_D the width of the die cavity, and respectively; R_{sP} section normalized radius of the punch this radius is measured in the xy plane, R_{sD} section normalized radius of the die measured in the xy plane, R_{fD} fillet normalized radius of the die measured in the xz plane, R_{fP} fillet normalized radius of the punch measured in the xz plane and S_P normalize punch travel (stroke). When we are dealing with rectangular cup, additional geometric parameters are considered, such as tL_P total length of the punch section, tL_B total length of the blank and tL_D total length of the die cavity. The parameters tL_P, tL_B and tL_D are similar to W_P, W_B and W_D used in the case of square cup but they measure the dimensions in the xz plane for rectangular cup geometry.

The blank is assumed to have frictional contact with the remaining parts. Due to the anisotropy of material behaviour, a 3D analysis has been considered modelling only a quarter of the deep drawing test is achieved. Adequate boundary conditions must be imposed at the symmetry axes. These symmetry axes are defined as the global X and Y axes in the FE mesh; the global Z axis is parallel to the punch displacement direction. The geometry of the FE model is that of the experimental process shown in Figure 1. The tools (punch, die and holder) are considered to be perfectly rigid and are modelled by rigid elements.

The structure is modelled using both 2D and 3D elements available in Abaqus. The blank sheet metal was modelled using eight-node continuum shell elements in Abaqus (SC8R) with reduced integration and one element through the thickness. The punch, die and blank holder are all modelled as 3 dimensional discrete rigid surfaces using four-node rigid surface elements (R_3D_4). In addition, the geometry has been variable, mesh parameters such as element size and mesh density may also be varied. This feature is needed to 'tune' the model in order to get mesh independent converged results.

5.2. Boundary conditions

As described in section 5.1 the DDP consist of two steps. During the second step, the punch moves at a constant speed V_P for a travel distance S_P with blank holder pressure P still applied. The die is fixed while the punch and blank holder are free to move in a direction normal to the blank plane. The double symmetry of DDP configuration is exploited and only a one-fourth of the assembly was modelled with symmetry boundary conditions applied at symmetry planes.

5.3. Numerical considerations

Mass scaling

At low punch speeds (and constant speeds) DDP is essentially a quasi-static process. Therefore, inertia forces do not play a major role and it is possible to speed up the convergence of the numerical solution using mass scaling. This approach requires

increasing the density of the material artificially in order to increase the stable time increment for the numerical integration. This procedure is termed "mass scaling". In the same manner as load-factoring this is an attractive method in instances where inertia plays a comparatively small part in the structural behaviour. As far as, in our case a blank forming analysis is considered, where a large proportion of the deformed structure is constrained by rigid surfaces and the kinetic energy of the blank itself is a small component of the overall energy balance of the problem, the mass scaling is applied to the blank only.

Thus, this is done by multiplying the density of blank material by a factor. This factor is chosen so that the solution time is reduced considerably all the while keeping the ratio of kinetic energy to strain energy of the blank low. A ratio of 0.05 is recommended [8] for best performance. Since the contributions of the die, punch and holder to inertia forces are negligible (the punch is moving at a constant speed) they were all assigned unit point masses. We have varied this factor from 500 to 60000 and several numerical examples were conducted to adjust this factor, so that we obtained converged solution while the ratio of kinetic energy to strain energy is kept less than 5% of the strain energy; a value of 10000 of the mass scaling have been used.

Contact parameters

The formulation of contact parameters between rigid surfaces (all the DDP tools except the blank) and a deformable body (which is the blank) is modelled with surface-to-surface model that is less sensitive to master and slave surface designations. In this formulation the finite sliding is undergo. However, the finite-sliding, surface-to-surface formulation with the path-based tracking algorithm do allow for double-sided surfaces used in this study. As far as, surface-to surface contact discretization has more continuous behaviour upon sliding, contact conditions with finite-sliding contact tend to converge in less iteration with surface-to surface contact discretization. In addition during all the parametric simulations, the analytical rigid surfaces are simulated by the master surfaces, slave surfaces are attached to deformable blank.

Friction coefficient parameter

Friction is one of the most important parameters affecting the material flow and the required load in forming process [9, 10]. FE investigations treating this parameter as a single parameter of DDP and drawing forming limit in sheet forming processes, are well précised in references [11] and [12].

In fact, friction has both positive and negative roles in metal forming. There are numerous instances where friction opposes the flow of metal in forming processes, and there are also several cases where the forming process is made possible by friction. A high value of friction between the blank and the matrix causes a significant thinning of the blank. On the opposite side by removing the lubricant, there appeared signs of damage at the contact surfaces materials.

5.4. Parametric simulation of the DDP

In DDP defects imply that the drawing of a cup has been completed but that the finished shape has some undesirable features in terms of geometry and/or mechanical properties. The defects fall into four main categories: (i) defects due to buckling, (such as wrinkling), (ii) defects due to asymmetrical flow (caring) (iii) surface defects, and (iv) distorted geometry in the unconstrained state (such as thinning).

The most primary defects that occurs in deep drawing operations are the over thinning and wrinkling of sheet metal materials. Generally, the thinning is produced in the blank wall compressed between the punch and the die; while the wrinkling is occurred in the flange of the blank. Those major defects are preventable if the deep drawing systems are designed properly.

The greater the die cavity depth, the more blank material has to be pulled down into the die cavity and the greater the risk of thinning and wrinkling in the blank. The maximum die cavity depth is a balance between the onset of wrinkling and the onset excessive thinning or fracture, neither of which is desirable. This balance is described with limit drown values commonly fixed by the industrial exigency, for example, in the automotive industry 20% of thinning in the sheet thickness is the maximum tolerable value.

In this parametric study, several parameters have been considered to be variable. For all the following cases, when ultimate thinning riches more than 30% of the initial blank thickness, the process is considered as failed. The simulations presented here are run with the following considerations: the material properties are those of MS material; the coefficient of friction are 0.02 for the Blank Holder contact, 0.02 for the Blank Die contact, 0.25 for the Punch Blank contact and then 0.03 for the global contact surfaces as follows, the punch speed is of 1.66 mm/s and the holder force is maintained at a value of 19.6 kN.

In order to assess the effect of parameters such as R_{fD}, R_{fP}, R_{sD}, R_{sP}, V_b, S_P, l_D and t_b on the DDP, we have adopted a simplified notation all the geometric parameters were done as a ratio to the final cross section width W_D; so that they can be dimensionless. The following ratios are then introduced:

$l_D = tL_D / W_D$, $s_P = S_P/W_D$, $r_{sD} = R_{sD} / W_D$,
$r_{sP} = R_{sP} / W_D$, $r_{fP} = R_{fP} / W_D$, $r_{fD} = R_{fD} / W_D$.

With the purpose of accomplishing this task, four parametric studies have been considered. In the first parametric study the effect of the aspect ratio (l_D) and the blank thickness on the limit of drawability of the DDP are considered. The second parametric study treats the effect of aspect ratio (l_D), the punch section radius (r_{sP}) and die fillet radius (r_{fD}) on drawability, wrinkling and percent thinning of the formed cup. The third parametric study examines the effect of the cup aspect ratio (l_D), die section radius (r_{sD}) and punch fillet radius (r_{fP}) on DDP. The fourth and last study is dealing with the effect of the aspect ratio (l_D) and punch travel distance (s_P) on the DDP A total of 136 finite element analyses cases have been used to carry out the described parametric study.

Effect of rectangular cup aspect ratio and blank thickness on drawability of the DDP

In this section, we are interested to attempt a correlation that describes the limits of drawability between the aspect ratios l_D, and the blank thickness t_b. In fact, to involve the relation between the initial blank thickness and the final aspect ratio of the rectangular cup; it is important to derive the trend of thickness variation along the particular path (the diagonal path highlighted with a red dashed line in Figure 4a. In this section study, thickness of the blank, t_b is varying in the range of 0.8 to 1.6 mm and the aspect ratios l_D is varying in the range of 1.2 to 1.6. The most important geometric parameters (rs_D, rf_D, rs_P, rf_P and w_D) are simultaneously; 0.3, 0.25, 0.1, 0.2, 40. Figures 8 to 10 are describing the thickness evolution vs. the diagonal distance for the

two limit aspect ratios. The variation of the thickness profile of the formed cup is measured in two ways. The first method is to evaluate the maximum thinning value which is expressed as:

$$p_t = \frac{t_b - \min\left(t_b\right)}{t_b} * 100 \qquad (2)$$

In this case the minimum is sampled over the diagonal path. The second method is to calculate the deviation of the final profile from the initial thickness this is expressed as:

$$\delta t = \sqrt{\sum_{k=1}^{N}\left(t_b - t_k\right)^2} \qquad (3)$$

where N is the number of sampling points along the diagonal direction and t_k is the thickness at the kth sampling point.

The x-axis of Figure 11a describes the different initial thickness of the blank, and the vertical axes define the values of the blank thicknesses after deformation along the diagonal path. From this graph, it is shown that the difference between the maximum and minimum thicknesses of the deformed blank is minimized for low initial thickness of the blank for the same geometric shape. The Figure 11b represent the group summery statistic table of the results for the ratios l_D=1.2.
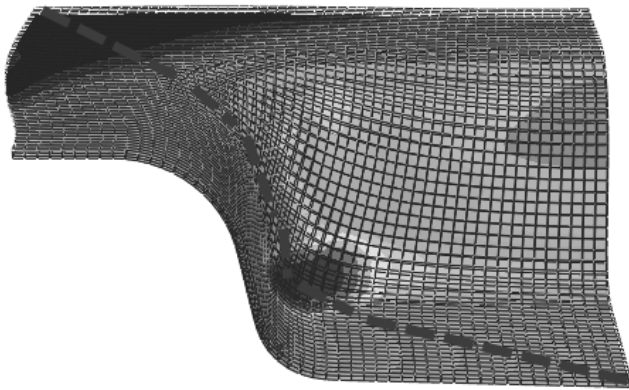
Fig. 8. A square rectangular cup with highlighted diagonal path
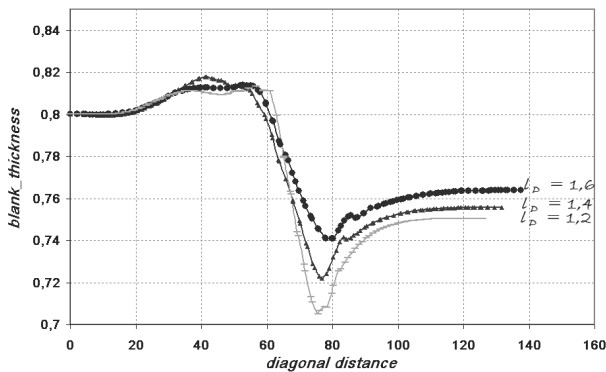
Fig. 9. Variation of the blank thickness along the diagonal path for various aspect ratios l_D and initial blank thickness t_b=0.8

Indeed, the dispersion indicator (standard deviation) varies from one sample to another depending on the group (the initial

thickness) otherwise exchange by value of the initial thickness. The same work is repeated for all the aspect ratio l_D as it is shown by Figure 12.
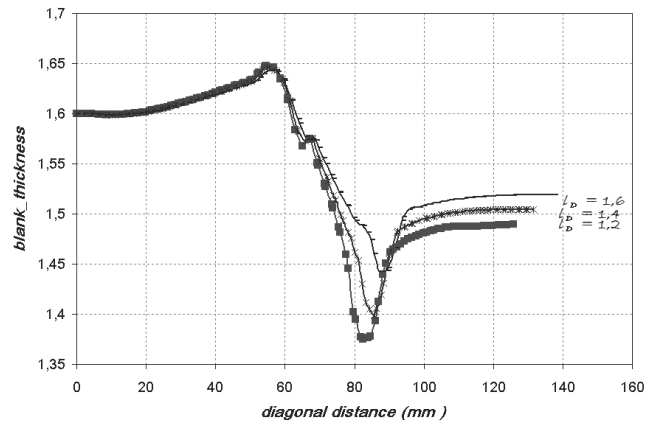
Fig. 10. Variation of the blank thickness along the diagonal path for various aspect ratios l_D and initial blank thickness t_b=1.6

a)

b)
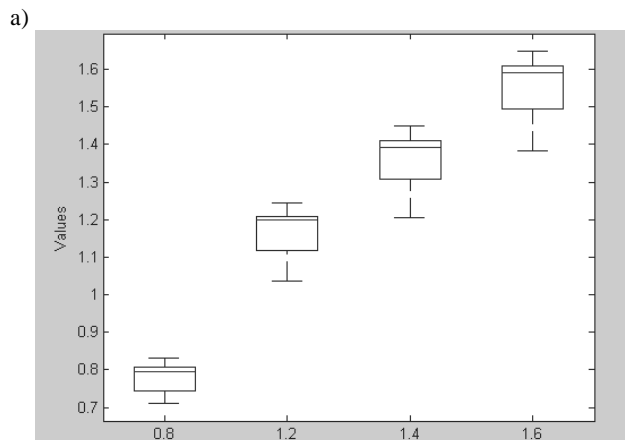
Group Summary Table			
Group	Count	Mean	Std Dev
0.8	118	0.7747	0.03781
1.2	120	1.16132	0.0582
1.4	118	1.3552	0.06633
1.6	118	1.5503	0.07265
Pooled	474	1.21017	0.06019
Bartlett's statistic	49.8482		
Degrees of freedom	3		
p-value	0		

Fig. 11. a) Variation of the blank thickness along of the deformed sheet for ratios l_D=1.2 and t_b=0.8, 1.2, 1.4, 1.6; b) summary of statistics results

Graphs in Figure 12 show that the variation of the thickness profile p_t and the deviation of the final profile δt increases when blank thickness t_b increases and also when aspect ratio l_D increases.

In the graphs represented by Figure 12, for the spectrum of l_D and t_b the trends of the thinning deviation curves measured by the δt parameter and those of the thinning variation are quite similar. In fact, the results show that the values of the maximum and

minimum of the thickness changes are minimized for smallest blank thicknesses and they are largest for highest aspect ratios l_D.

From Figure 12, it is established that the rate thinning defined as the aspect of the maximum thinning to the blank thickness t_b is depending on the aspect ratio l_D. It seems that as much as the aspect ratio l_D is low, the maximum thinning rate is upper. Thus, the rate of maximum thinning is slowed down by the increasing of the final cup aspect ratio l_D. Results show that, varying the aspect ratio l_D from 1.2 to 1.6 has reduced the thinning of the blank thickness by 30% for the same blank thickness of 1.6 mm.
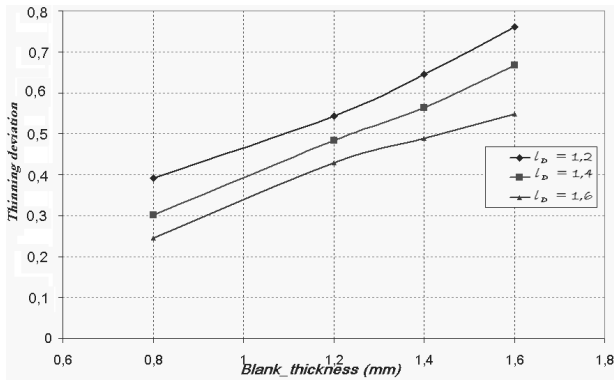
Fig. 12. Thinning deviation of the thickness distribution along diagonal path versus the blank thickness t_b and aspect ratio l_D

Effect of die fillet and punch section radii on drawability of the DDP

In this section we are dealing with the study of the geometric parameters such as the punch section radius (r_{sP}), the die fillet radius (r_{fD}), and their interaction with the aspect ratio l_D, on the drawability of the DDP. In fact, several finite element analyses were performed, 36 FEA experiments are done with l_D, which rises between 1 to 1.5, r_{sP} is varying between 0.2 to 0.8 and r_{fD} between 0.4 to 0.8. For the entire calculations in this section the normalized punch stroke s_P is fixed to 0.75, the blank thickness t_b is fixed to 1.2.
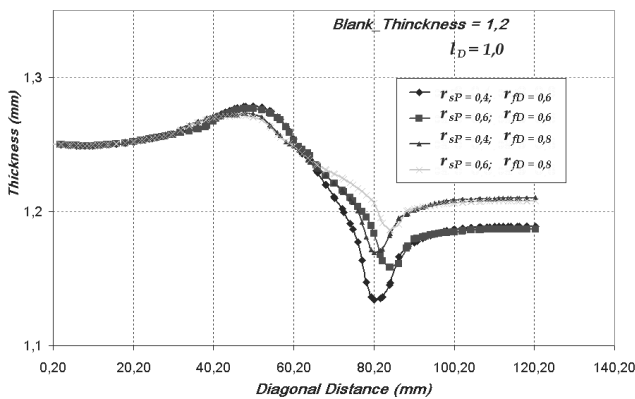
Fig. 13. Variation of the thinning along the diagonal path for various aspect ratios r_{sP} and r_{fD}

From Figure 13, it seems that when r_{sP} takes minim values; the growth of maximum thinning is well emphasized. By the way, in Figure 13 it is noticed that as much as r_{fD} and r_{sP} are declines;

the maximum thinning trends to decrease. Figure 14 represents the thinning deviation along the diagonal path, for various aspect ratios l_D and punch section radius (r_{sP}).We note that the trend of thinning deviation is closely similar to the trend of maximum thinning vs r_{sP}. In fact, the increase of the final cup aspect ratio l_D induces decrease of the maximum thinning independently from (r_{sP}). Figure 15, show that above $r_{sP} = 0.4$, the increase of l_D ratio leads almost to increase of the maximum thinning. It is thus noticed that we have to avoid high r_{fD} parameters combined with high r_{sP} parameters, especially with thick sheet blanks, because it leads to greatest maximum thinning.
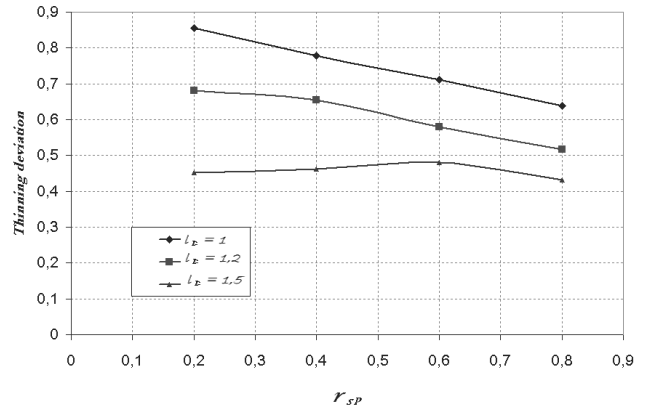
Fig. 14. Variation of the thinning deviation along the diagonal path for various r_{sP} and l_D
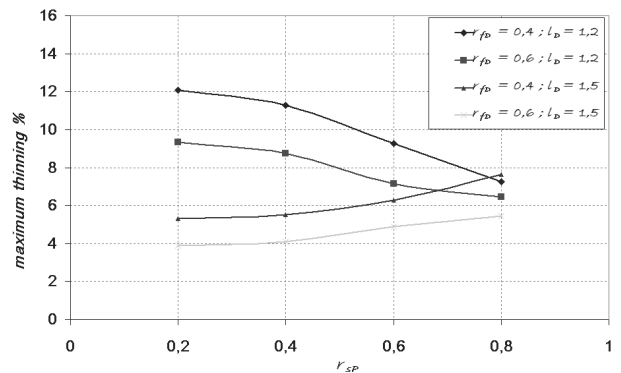
Fig. 15. Variation of the maximum thinning along the diagonal path for various r_{sP}, r_{fD} and l_D

Effect of punch fillet and die section radii on drawability of the DDP

In some literature review [13], [14] and [15], the effect of the punch fillet radius was considered as effective parameter which can influence the drawability of the DDP. Nevertheless, interaction between punch fillet radius (r_{fP}) and die section radius (r_{sD}) has not been well discussed. In this paragraph we will elucidate the effect of interaction between those parameters. We will focus on the impact of this interaction on DDP and highlight the change in the behaviour of the maximum thinning according to variation of the parameters; aspect ratio l_D and t_b.

A series of 64 FEA experiments is done by varying the blank thickness in the range from 1.2 to 1.6 mm, the aspect ratio l_D from

1.2 to 1.6, the die section radius from 0.3 to 0.8 and the punch fillet radius from 0.1 to 0.22, the punch stroke s_P was kept constant and equals to 0.75.
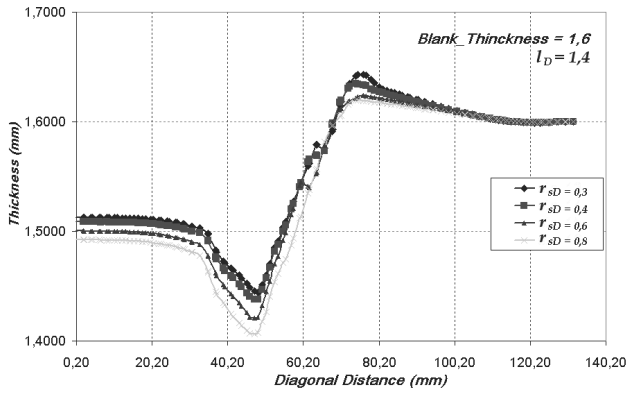
Fig. 16. Variation of the thickness along the diagonal path for various r_{sD} for $l_D=1.6$ and $t_b=1.4$
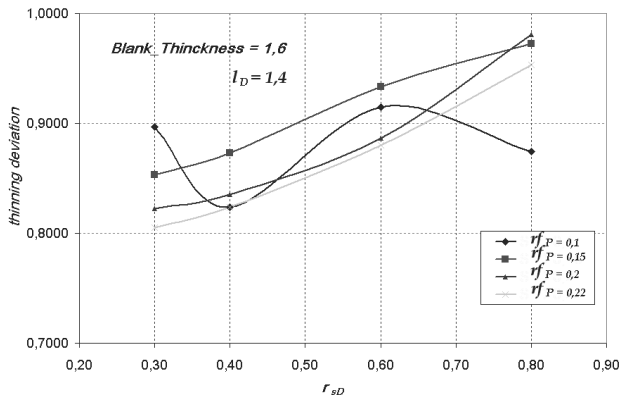
Fig. 17. Variation of the thinning deviation along the diagonal path for various r_{sD}, and r_{fP}. For $l_D=1.4$ and $t_b=1.6$
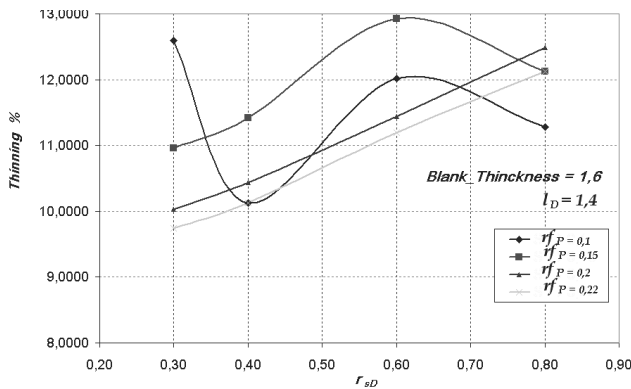
Fig. 18. Variation of the maximum thinning % along the diagonal path for various r_{sD}, and r_{fP}. For $l_D=1.4$ and $t_b=1.6$

According to Figure 16 it is observed that, the maximum thinning for the different r_{sD} ratios is located at the same zone which corresponds to the corner of the cup. Figure 17 introduces the

thinning deviation versus r_{sD} for different values of r_{fP}. The thinning profile is generally growing, according to increasing of the r_{fP} for the same aspect ratios l_D and r_{sD}. Results confirm that the lower r_{fP} is, the more severe maximum thinning is. In fact, it is observed that interaction between r_{fP} and r_{sD} is well emphasized for a relatively thick blank ($t_b=1.6$ mm). In addition, values of r_{sD} larger than 0.6 improve the critical thinning, when the punch fillet radius is smaller than 0.1. This result is very significant; in fact a high value of the fillet punch radius > 0.1, combined with section die radius < 0.6, leads to a minimum thinning Figures 18, 19 and 20.

Figure 20 shows the large amount of thinning localized in the critical zone of the diagonal path when we move from $t_b=1.2$ to $t_b=1.6$.
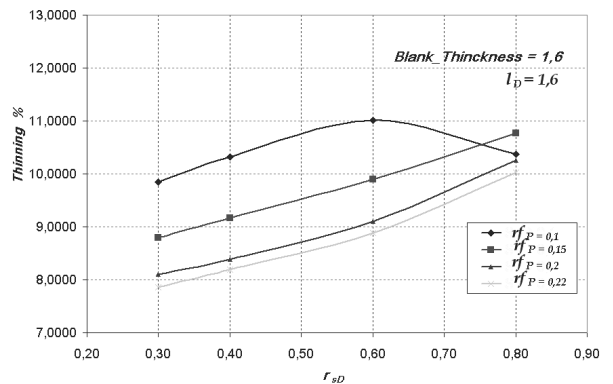
Fig. 19. Variation of the maximum thinning % along the diagonal path for various r_{sD}, and r_{fP} for $l_D=1.6$ and $t_b=1.6$
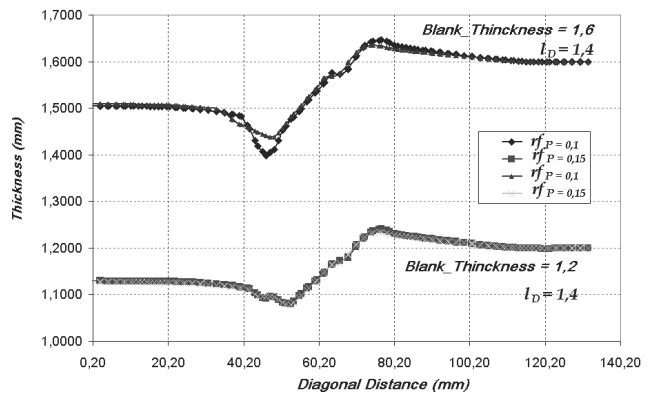
Fig. 20. Variation of the thickness along the diagonal path for various r_{fP} for $l_D=1.4$ and $t_b=1.4$; 1.2

The effect of interaction between r_{sD}, r_{fP}, l_D and t_b is presented by Figures 21 to 23. A significant sensitivity to the interaction between the r_{sD}, r_{fP}, with l_D and t_b, is noticed on the thinning profile.

We kept the initial blank thickness constant and equal to $t_b=1.6$ mm, then we have varied the final cup aspect ratio l_D from 1.2 to $l_D=1.6$. According to Figure 21, the thinning deviation for the different values of r_{sD} has been distinguished with a significant reduction. Figure 22 confirm that when the final cup aspect ratio l_D increases, the maximum thinning with the same r_{sD}, r_{fP}, is slowed down. The growth of r_{fP}, parameter is accompanied with the decrease of maximum thinning, but this maximum thinning has to grow for increasing r_{sD} values.

In the cases with thin initial blank t_b=1.2, it appears that for the entire studied cases from Figures 20 and 21, the maximum thinning profile tends to take a rapid rate reduction within the increase of r_{sD} parameter. This fact is particularly noted for r_{sD} above 0.6.
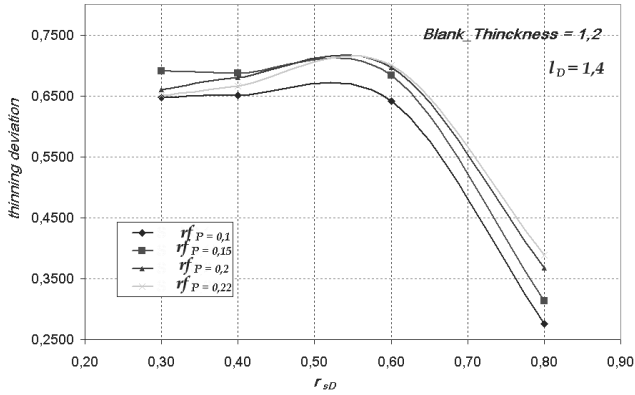
Fig. 21. Variation of the thinning deviation along the diagonal path for various r_{sD}, and r_{fP} with l_D=1.4 and t_b=1.2
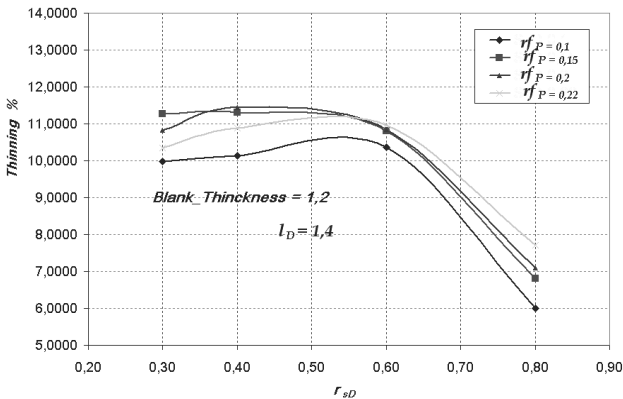
Fig. 22. Variation of the maximum thinning % along the diagonal path for various r_{sD}, and r_{fP} for l_D=1.4 and t_b=1.2
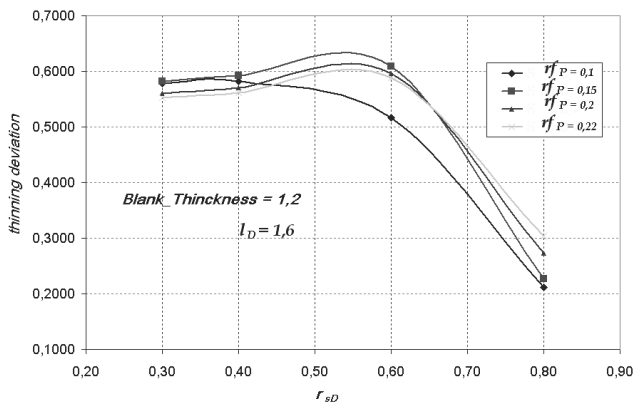
Fig. 23. Variation of the thinning deviation along the diagonal path for various r_{sD}, and r_{fP} for l_D=1.6 and t_b=1.2

From Figures 22 and 23, it appears that for larger aspect ratio l_D, the thinning deviation and the maximum thinning are being decreasing. We note at least, that above r_{sD} =0.6, even though the maximum thinning is slowed down, the increase of r_{fP} ratio leads to a small growth of the maximum thinning instead of decreasing.

Sensitivity to the Punch travel

In order to take advantage of this parametric FEA study, the interaction between the l_D aspect ratio and the punch travel s_P ratio are emphasized in Figures 24 to 28. Four values of parameter s_P are experimented at constant value of l_D; then the analysis is repeated for a different value of l_D. It appears that for a square cup the growth of the s_P doesn't lead to the increase of the maximum thinning. In fact, as it is mentioned by Figure 28, beyond s_P=0.6 the increase of the punch travel slow down the maximum thinning of the square cup. Conversely, under 0.6 of the s_P value, the growth of the ratio s_P leads to a rapid increase of the maximum thinning. This paradoxes result can be attributed to the fact that a friction of the sheet between the blank holder and the die is almost important so that a higher thickening is observed for the flange of any rectangular cup characterized with a s_P above 60% of the blank cross section width. Therefore, when the punch travel increases, a uniform distribution of the thickness can be transferred from the thickening amount of material. The critical thinning is being slowed at the end of the process.
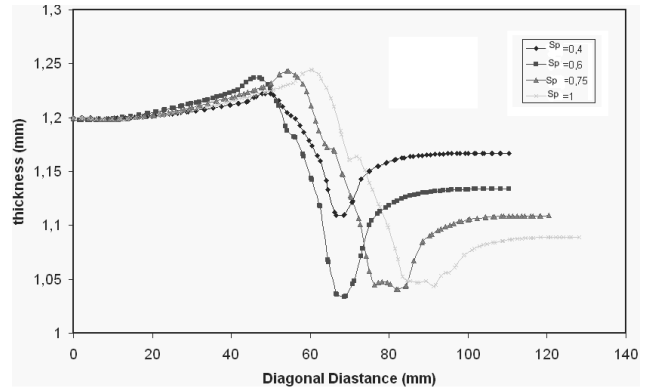
Fig. 24. Variation of the thinning along the diagonal path for various aspect s_P and l_D=1
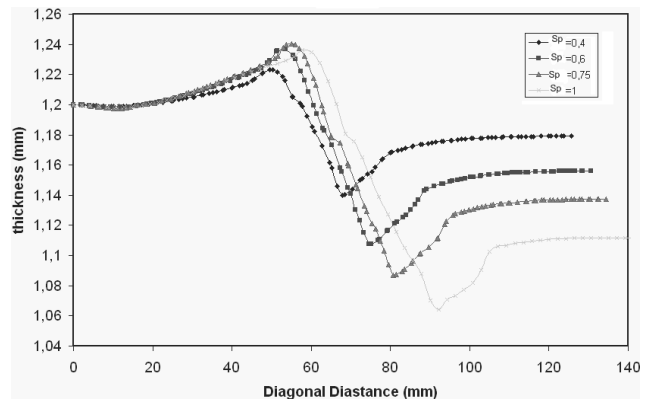
Fig. 25. Variation of the thinning along the diagonal path for various aspect s_P and l_D=1.5

Figures 26 to 28 show that maximum thinning increased with s_P for cups with l_D larger than unity. Beyond a punch travel equals to the blank width of the cross section, some wrinkling can be observed at the vicinity of the corner section as highlighted by Figure 27, this fact is considered as major failure. Figure 28, illustrate two important facts; the larger the aspect ratio l_D is, the smaller the maximum thinning for the same s_P. Indeed, as well as the aspect ratio l_D is higher, the maximum thinning trends to grow linearly.
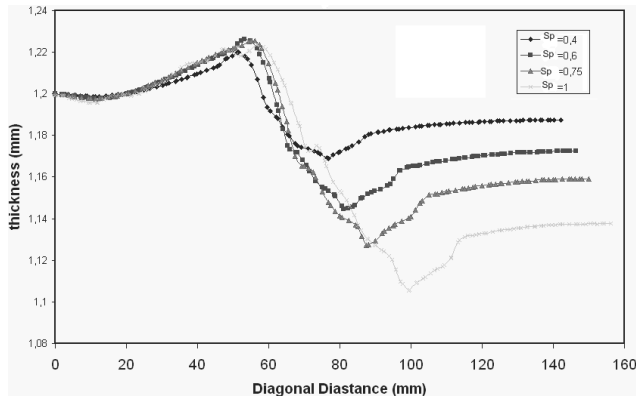
Fig. 26. Variation of the thinning along the diagonal path for various aspect s_P and $l_D = 2$
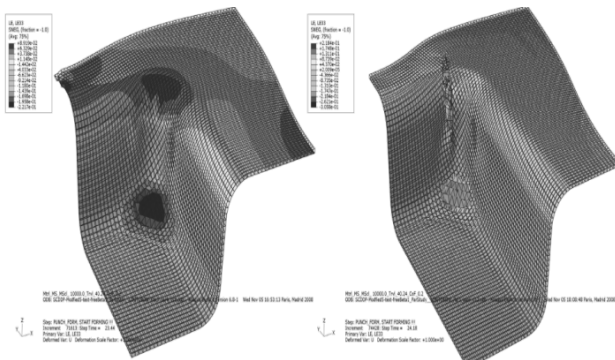
Fig. 27. Plastic deformation out in the thickness direction for the following cases $s_P = 1$ and aspect ratio, $l_D = 1.5$ and 2 respectively
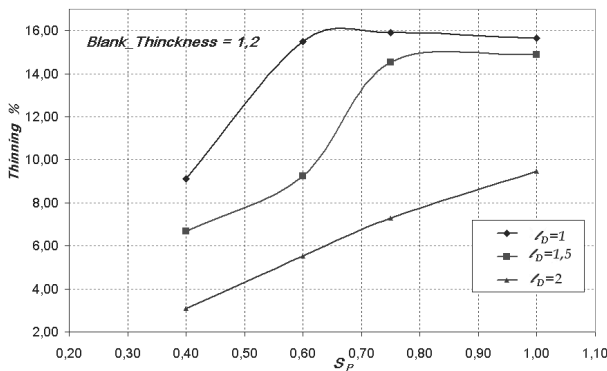
Fig. 28. Variation of the thinning versus the s_P for various aspect ratio l_D

5.5. Discussion

FE analysis results show that localized deformation and wrinkling occur along the major axis of diagonal DD when interaction between some of the geometric parameters is hold as detailed in section 5. This is attributed to the non-uniform contact in the cross-section between the mid-blank and the punch during the forming process. With compared results between the various couple of geometric parameters (radius of the punch and the die), it was confirmed that for a selected value of the final geometry of the blank (l_D), we can associate particular values of punch section and fillet radius to avoid wrinkling and tearing of the blank. In fact, if the choice of the following parameters $r_{sP} = R_{sP} / W_D$, $r_{fP} = R_{fP} / W_D$, $r_{fD} = R_{fD} / W_D$ is not compatible different an excessive thinning can occurred and lead to a tearing. As it is known, tearing in the drawing mode occurs when the tensile flow stress at a local neck exceeds the ultimate stress. In such location the strain takes also its ultimate value and then it could be considered as a forming limit. This important consideration for general rectangular cross sections, has been incorporated by FE DDP forming sequence, in which we maintain a punch speed constant for the entire cases and we change the contact section between punch, blank and die with a sensitivity analysis for rectangular cups to the various combination of fillet and sections radius which in turn minimizes the maximum thinning.

In section 5, a limit of drawability according to aspect ratio l_D blank thickness t_b is considered by controlling the material flow and avoiding necking at the bottom corners of rectangular cup. If r_{sD} and r_{fP}, are too small, sheet material does stick to the die and cannot flow easily to the die cavity. This could be associated to a failure of the process; (wrinkling and excessive amount of thinning).

As it was indicated, for larger aspect ratios l_D, smaller initial sheet blank thicknesses, the maximum thinning are being decreasing. But, we note that above $r_{sD} = 0.6$, even though the maximum thinning is slowed down with conditions above, the increase of r_{fP} ratio leads to a small growth of the maximum thinning instead of decreasing. Indeed, great value of the r_{fP} ratio above 0.7 can lead to the development of local wrinkling phenomenon.

6. Optimisation FEM study

Simulations of forming processes are increasingly used by large and small companies in the early stage of a product design. These simulations have become indispensable for the development of products and the automation of this process itself.

Optimization of parameters such as die radius, blank holder force, friction coefficient, etc., can be accomplished based on their degree of importance on the sheet metal forming. In this investigation, a statistical approach called optimization mon-objective method has been applied to design the process providing the best geometric parameters which lead to the selected minimum failure criterion.

6.1. Summery of some parametric FE results and discussion

The aim of this section is to outline the most important results presented in section 5, in order to summarize the principle geometric parameters that were the mostly affecting the drawability

of the final product. In fact, after studying the effect of different geometric parameters (r_{sP}, r_{fD}, r_{fP}, r_{sD}, l_D, s_P and t_b) on the forming process and more specifically on the thinning phenomenon and the thickness distribution along the critical diagonal path as mentioned by Figure 8a the following conclusions were underlined:

- within a fixed value of the final geometry of the deep drawn rectangular cup (w_D, l_D), it is possible to associate particular values of section and fillet radius of the punch r_{sP} to avoid wrinkling and tearing of the blank;
- if r_{sD} and r_{fP} are too small, the material of the sheet sticks to the die and cannot flow easily into the cavity of the die which leads to the possible existence of wrinkles and excessive thinning, leading to the failure of the forming process;
- for large values of l_D, and low values of initial blank thickness t_b, the maximum thinning decreases. But beyond r_{sD}=0.6, and with the increase of the r_{fP} it is noted that we have an increase of the maximum thinning. In fact, within a ratio r_{fP} greater than 0.7, local development of wrinkling phenomenon is developed;
- increasing of r_{sD} usually causes the decrease of maximum thinning, but a low value of punch fillet radius r_{fP} associated with a high value of blank thickness t_b leads to the thinning increase, so that local wrinkles can appear on the blank sheet;
- increase of punch stroke s_P for rectangular initial blank sheet causes the existence of thinning. For values of punch stroke above the section width of the blank, some wrinkles may appear at the corner of the final geometry of the sheet metal.

6.2. Statistical analysis results of the FE model

The FE numerical simulation of forming process such as drawing process can provide a large amount of final drown configurations based on multiple combinations of the different variable parameters of the model. To optimize the model behaviour and also to save cost of the big amount of time calculation, it is almost versatile to hold up with statistical techniques. In fact, statistical computing is essential when seeking optimized solution to reduce costs and manufacturing time. This kind of calculation is actually done using the well known statistical Matlab tool box.

The statistical study is based on the calculation of certain statistical parameters such as: (mean, variance, standard deviation, median, correlation.) and summaries results with standard graphics (histogram, box plot, chart points ...).

Indeed, the interest of statistical representations lies in the fact of presenting the influence of several variables in a well extended spectrum of values; against a limited one as in it was described in the parametric study for described in the previous section.

6.3. Statistics problem

The graphs of variations in thickness and thinning rates presented in the previous section 5, gives a general idea on the deep drawing model behaviour within variation of various parameters. Indeed, the interpretations were based on the decrease or increase of the thickness and rate of thinning of the blank without calculating the limit deviations of such variations. Using mathematical tools such statistical appropriate functions, we have interpreted statistically numerical results defined in the section 5. The statistical study is based on the calculation of certain

statistical parameters such as: the mean, variance, standard deviation, and dispersion. In fact, the interest of statistical representations lies on the fact that the lecture and interpretation of those results according to statistical variables give a best meaning and enhance enlightenment.

Cases study of the forming problem

The function chosen to perform the statistical study is called "vartestn" via to the statistical Matlab toolbox. It allows the calculation of certain statistical parameters, comparison of variance of multiple samples using Bartlett's test with a graphical representation.

The synthax parameters are as follow, vartestn (X), vartestn (X, group), P = vartestn (...) are defined such as:

- vartestn (X): using the Bartlett test to check the equal variance for the columns of the matrix X. Indeed, this is a test of the null hypothesis H0 that postulate that the columns of the matrix X are of a normal distribution with the same variance, against the alternative hypothesis Ha with columns of the matrix X of even distribution which have different variances. The result is displayed in graphical form with a table that contains the values of statistical parameters;
- vartestn (X, group) requires a vector argument X and a group which can be variable, a vector row of character with one row for each element of the matrix X. The values of the matrix X are in the same group. This function tests the homogeneity of variance in each group;
- P = vartestn (...) returns the p-value, i.e. the probability of observing the given result when the null hypothesis of homogeneity of variances is true. In cases where this value is very small, there is a doubt on the validity of this hypothesis.

Effect of the blank geometric shape and thickness t_b on the forming process

In the following example we set l_D =1.2 mm and it has changed the value of the initial thickness of the blank t_b in the rage of (0.8, 1.2, 1.4, 1.6). Taking into account all these data, we obtain the results shown by Figures 29a and b.

The graphic representation illustrated by Figure 29b consists on a schematic rectangular representation called "box plot". This representation is one way to approach the statistics summery concepts. In fact, it can summarize data in a very visual outcome see Figure 29 and easily compare various statistical variables. This representation is located in a two landmark axes; the samples group, axis and the axis containing all values of the samples. For each group, a "box plot" which presents some statistical parameters such as:

- the middle – it divides the data into two equal sets;
- quartile – the quartiles of statistical series are the three values Q_1, Q_2 and Q_3 of character who share the population into four parts of the same size;
- the inter-quartile range – the difference between the upper and lower quartiles (Q_3 - Q_1) and also indicates the dispersion of a dataset;
- group – group of diffrent t_b variables;
- count – number of values in the vector t_b: (thickness values along the diagonal path), this number is also the length of the vector thickness t_b;
- STd – standard deviation: $S = \sqrt{\sum_{i=1}^{N} \frac{(xi - m)^2}{N-1}}$;

- mean – mean value of each group that is defined with the folowing equation:; $m = \sum_{i=1}^{N} \frac{xi}{N}$

- Barletts statistic: statistical test of Barlett

$$T = \frac{(N-k)\ln S_p^2 - \sum_{i=1}^{k}(N_i -1)\ln S_i^2}{1 + (1/3(k-1))(\sum_{i=1}^{k}(1/N_i -1) - 1/(N-k))}$$

with: S_i^2 – the variance of ith Group, N – total length of the discretized and weighted simples, N_i – length of the vector corresponding to the group i, k – group's number, S_p^2 – pooled variance: mean weighted of the group variance

$\sum_{i=1}^{k}(N_i -1)S_i^2$

Variances are considered unequal if T> $X^2_{(\alpha,k-1)}$ with $X^2_{(\alpha,k-1)}$ is the biggest critical distribution of Chi square (α=significant threshold, k-1: degree of freedom, and k is the number of samples).

- P-value – is related to α (for great values of P, the hypothesis H_0 is true, otherwise this hypothesis is false).

a)

b)
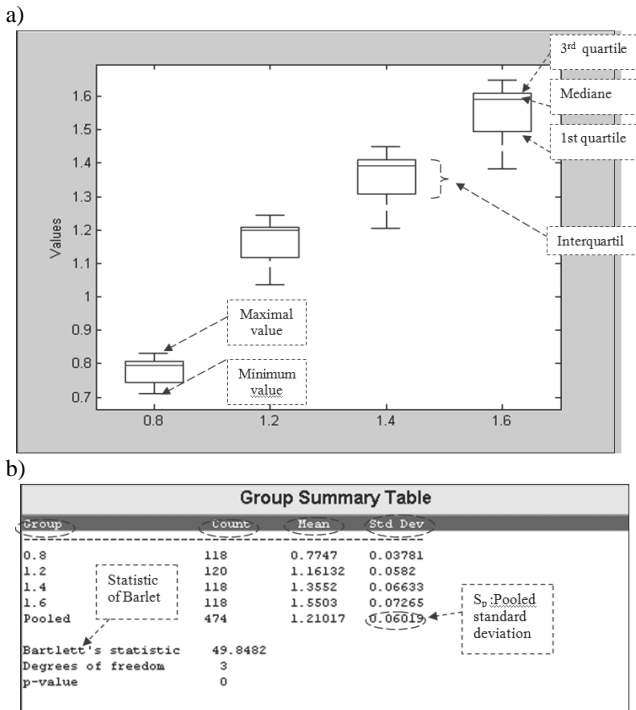
Fig. 29. a) Thickness variation of the blank with l_D=1.2 and t_b=0.8; 1.2; 1.4 and 1.6 mm; b) summary table thickness variation of the blank with l_D=1.2 and t_b=0.8; 1.2; 1.4 and 1.6 mm

In Figure 29a, the x-axis which represents the different groups, defines the initial blank thickness t_b, and the y-axis values represent the different thickness ranges of the blank along the diagonal path during the forming process. From this graph, we see that the difference between the maximum and minimum thickness of the blank at the end of the process along the diagonal path is almost obtained with law thicknesses of the blank. Indeed, for t_b=0.8 mm, we notice that the stamped sheet metal has undergone less thinning much lower than it is for the other t_b cases. From Figure 29b we notice that the p-value is equal to 0, which is lower

than the risk of error α (0.05), this fact confirms that the hypothesis H_0 is well justified. Certainly, the indicator of dispersion (standard deviation) varies from one sample to another depending on the group, so according to the value of the initial thickness of the blank t_b. Therefore, the samples presented in Figure 29b haven't the same variance. It is concluded that for rectangular final geometry of the blank with $l_D > 1$, and with initial law thickness t_b, there is important thinning of the deformed blank.

Effect of the section radius of the punch r_{sP} parameter on the blank thinning rate

In order to visualize the influence of r_{sP} parameter on the thickness distribution of a blank, we have considered different values r_{sP} with for the t_b varying in the range from 0.2 to 0.8 and an aspect ratio equals to 1.2. Results are then obtained with Matlab as shown it in Figures 30a and b.

a)

b)
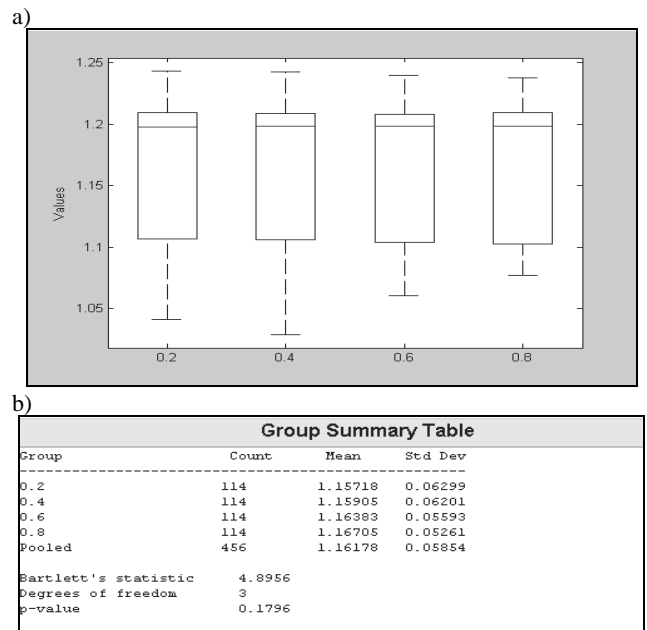
Fig. 30. a) Thickness variation of the blank with l_D=1, t_b=1.2 and r_{sP}=0.2, 0.4, 0.6 and 0.8; b) summary table for the same conditions as in Figure 30a

The results presented in Figure 30a show that the 4 samples of the parameter r_{sP} have almost the same inter-quartile; we can say that they are compatible for a certain range of thickness. We have noticed from the value p-value (Figure 30b) that also the same samples have the same variances. We also note from these figures that as far as the parameter r_{sP} decreases the thinning of the final blank sheet increases. In conclusion, the thinning rate is high for low values of r_{sP} in the case of a square plate and initial thickness t_b=1.2 mm.

Effect of the fillet radius of the die r_{fD} parameter on the blank thinning rate

In this example, we will study the influence of the r_{fD} variation on the thinning rate of the blank for a square initial sheet blank with t_b=1.2 mm. In this case r_{sp}=0.4, l_D=1 and t_b=1.2 mm, r_{fD} is varying from 0.4 to 0.8. We obtained the following results (Figure 31).

a)

b)

Group Summary Table			
Group	Count	Mean	Std Dev
0.4	114	1.1656	0.05367
0.6	114	1.17378	0.0418
0.8	114	1.18316	0.0291
Pooled	342	1.17418	0.04272
Bartlett's statistic	39.9279		
Degrees of freedom	2		
p-value	0		
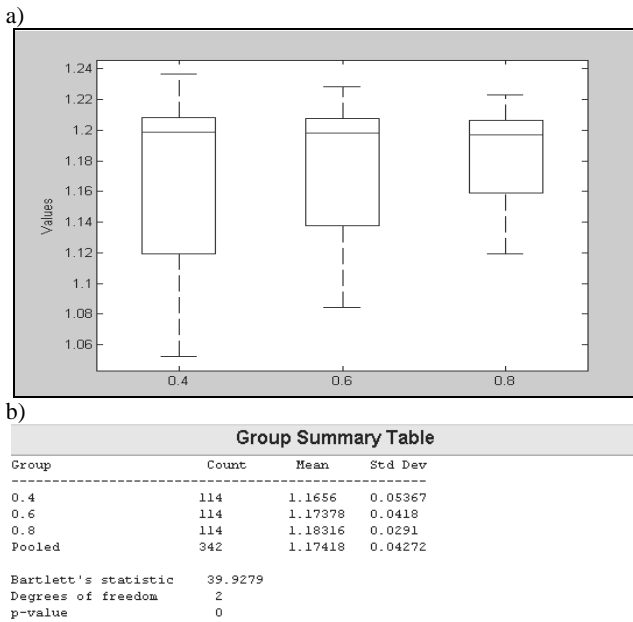
Fig. 31. a) Blank thickness for r_{fD}=0.4, 0.6 and 0.8 with r_{sP}=0.4, l_D=1 and t_b=1.2 mm; b) group summary table of data related to the Figure 31a

It is concluded from Figure 31, that the lowest mean value is (1.1656) that is corresponding to the 1st group (r_{fD}=0.4). We notice that according to this statistical parameter, the highest thinning is found for r_{fD}=0.4, we can also notice that as far as this parameter increases the thinning is spectacularly diminishing. We can conclude that with a square DDP with initial blank thickness of 1.2 mm more the parameter r_{fD} increases, more the thinning is decreasing.

Effect of the section radius of the die r_{sD} parameter on the blank thinning rate

From Figure 32a, we can see that the formed metal reaches a maximum rate of thinning (thickness <1 mm) for r_{sD}=0.4. In conclusion, for a square plate, more the parameter r_{sD} increases, there is a chance to get important thinning.

Figure 33a shows that the minimum variations in thickness corresponds to r_{fD}=0.2. We can conclude that a high value of r_{fD} minimizes the risk of excessive thinning leading to failure.

7. Description of optimisation problem

The improvement and the cost reduction in forming process products has been always a major objective in automotive industry.

In a forming process, the sheet metal is subjected to mechanical tools action; punch, die and blank holder. These tools are generally considered as rigid bodies, causing contact actions, the deformation of the sheet along a well defined kinematic. The normal and tangential interactions due to contact between tools and sheet metal are taken into account. The coefficients of friction blank-tools have a great influence on the process development and its quality. Taking into account all these considerations and from finite element

a)

b)

Group Summary Table			
Group	Count	Mean	Std Dev
0.2	114	1.15878	0.06071
0.25	114	1.15824	0.06062
0.4	114	1.15355	0.06289
Pooled	342	1.15686	0.06142
Bartlett's statistic	0.1968		
Degrees of freedom	2		
p-value	0.9063		
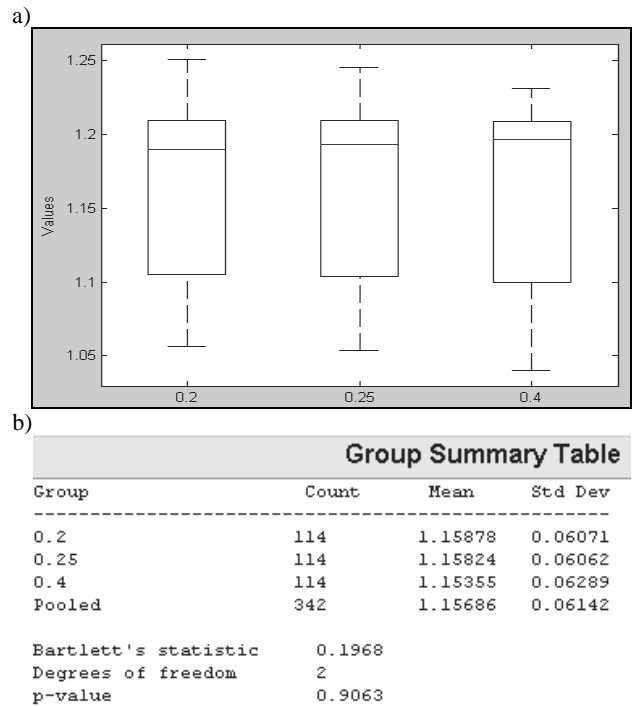
Fig. 32. a) Blank thickness for r_{sD}=0.4, 0.6 and 0.8 with r_{fP}=0.4, l_D=1 and t_b=1.2 mm; b) group summary table with blank thickness for r_{sD}=0.2, 0.25, 0.4, r_{fP}=0.1, l_D=1 and t_b=1.2 mm

a)

b)

Group Summary Table			
Group	Count	Mean	Std Dev
0.1	114	1.15824	0.06062
0.2	114	1.15717	0.06299
0.4	114	1.16529	0.05324
Pooled	342	1.16023	0.0591
Bartlett's statistic	3.3997		
Degrees of freedom	2		
p-value	0.1827		
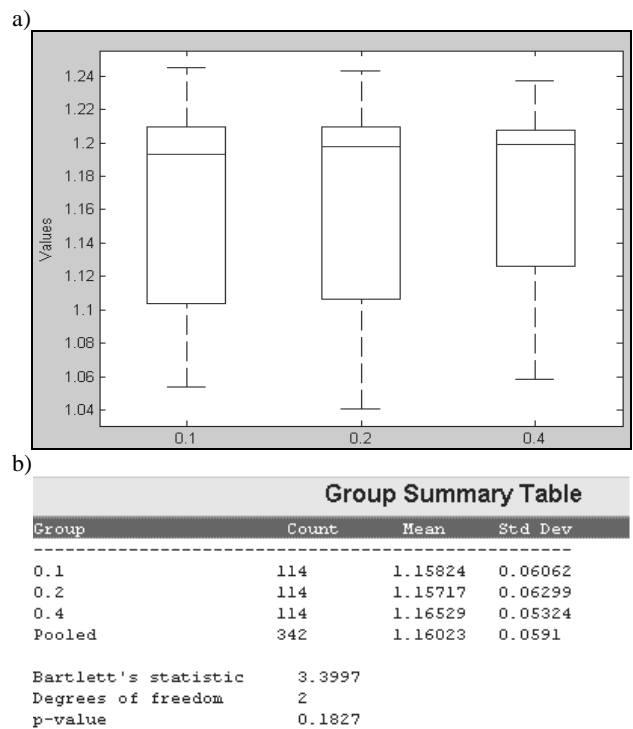
Fig. 33. a) Variation of r_{fP}=0.1, 0.2, 0.4 with r_{sD}=0.25, l_D=1 and t_b=1.2 mm; b) group summary table

calculations performed by Abaqus, we used the values of blank thickening in deep drawing along the diagonal path of sheet metal to judge the quality and the acceptability of the final formed product. In this study, a criterion of maximum thinning tolerance of 20% is adopted. We chose this criterion because the risk of developing structural defects resulting from thinning as, wrinkles, breaks, tears, is mostly high when thinning reaches 20%. However, according to formatting examples presented in the previous section, the numerical predictions are far from experimental realities. For this reason, we chose an approximation method for optimization of geometrical parameters of the drawing process such as the different radii of the die and the punch.

7.1. Results and discussion

After studying the effects of different geometric parameters such as (r_{SP}, r_{FD}, r_{fp}, r_{sD}, l_D, and S_P, t_b) on the forming process, specifically on the thinning phenomenon and the thickness distribution along the critical diagonal path; the following conclusions are considered:

- according to a final geometry dimension of the clank l_D, we can associate particular values of the tools radii to avoid wrinkling and tearing of the blank. In fact; several Remarque's are underlined;
- if r_{fp} is too small, the material of the sheet sticks to the die matrix and cannot flow easily into the of matrix cavity, which leads to the appearance of wrinkles and excessive thinning;
- for large values of l_D, and low values of initial blank thickness t_b, the maximum thinning decreases. But for $r_{sD}=0.6$, and with the increase of r_{FP} thinning was growing up instead of decreasing. A radius r_{fp} smaller than 0.7 leads to the development of local wrinkles;
- the fact of increasing r_{sD} usually causes the decrease of maximum thinning;
- a low value of the fillet punch radius r_{fp} associated with a high value of blank thickness leads to increased thinning and the possible appearance of wrinkles;
- increase of S_p for rectangular plates causes the appearance of thinning. For values of punch travel above the section width of the blank, some wrinkles may appear at the corner of the sheet metal after forming.

On the light of these interpretations we have reviewed the following examples to show the thinning distribution of the final formed product according to highlight the particular combinations of geometric parameters that can lead to excessive thing and wrinkling.

Effect of r_{sD} and r_{fP} on the forming process

$r_{fp}=0.2$; $r_{sD}=0.3$; $t_b=1.2$; $l_D=1.4$: law values with r_{fP} and r_{sD}, we have reported that for $r_{fP}>0.1$ and $r_{sD}<0.6$ we have less thinning and les wrinkling as shown by Figure 34 with $r_{fP}=0.2$; $r_{sD}=0.3$; $t_b=1.2$; $l_D=1.4$.

Effect of r_{fD} and r_{sP} on the forming process

In this case, we have considered the simulation of the following parameters: $r_{fD}=0.6$; $r_{sP}=0.7$; $t_b=1.2$, $l_D=1.2$, with high values of parameters r_{sP} and r_{fD}, it is shown that the thinning is more important in this case (Figure 35).

$r_{sP}=0.4$, $r_{fD}=0.6$, $t_b=1.2$ and $l_D=1$, for a square blank sheet with law values of the parameters r_{sP} and r_{fD} on a reduction of thinning according to Figure 35 is shown in Figure 36.
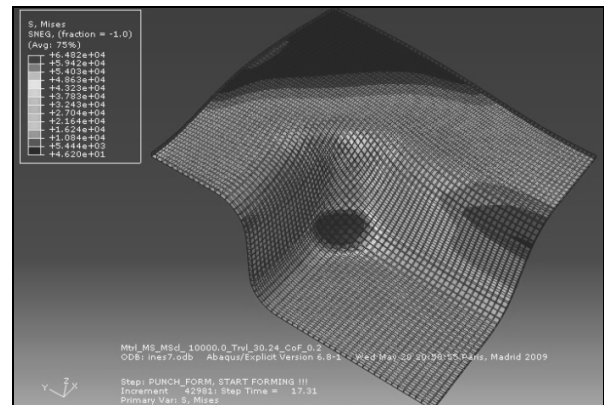
Fig. 34. DDP of a rectangular profile
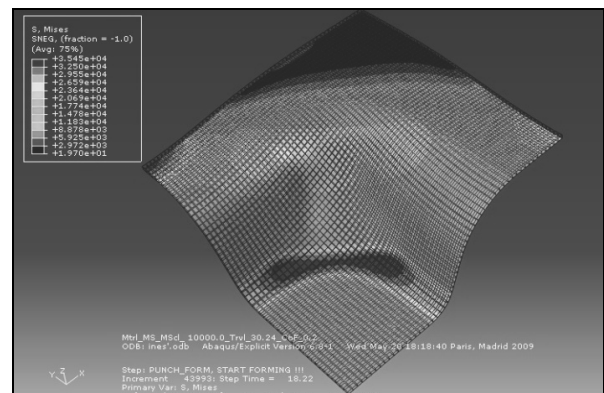
Fig. 35. High thinning with $r_{fD}=0.6$; $r_{sP}=0.7$; $t_b=1.2$, $l_D=1.2$
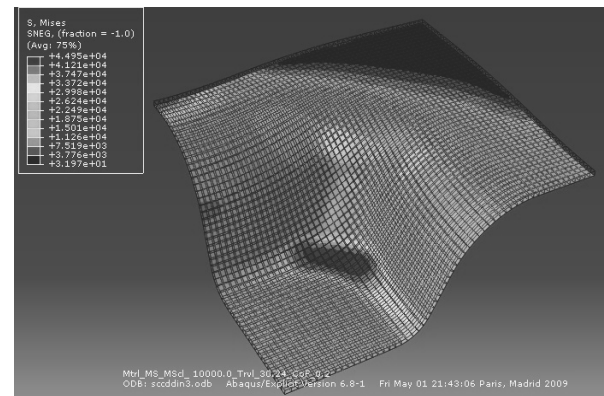
Fig. 36. Thinning reductions in the critic path; $r_{sP}=0.4$, $r_{fD}=0.6$, $t_b=1.2$ and $l_D=1$

8. Optimisation problem of the DDP

8.1. Optimisation method

Basic concept of optimization techniques

The mathematical concept of optimization is presented by Figure 37. It is composed mainly of two key phases: modelling

and solving the optimization problem. The modelling phase consists of:

1. selecting a number of variables where the user is authorized to adjust,
2. choosing an objective function,
3. taking into account the possible constraints.
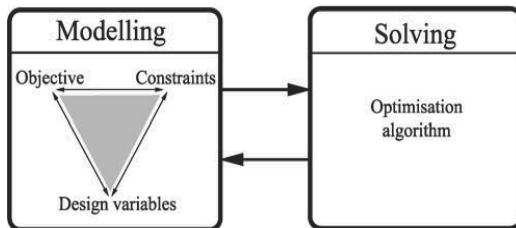
Fig. 37. The concept of basic mathematical optimization [16]

According to [15], most research has focused on solving some optimization problems, where the selection and application of an optimization algorithm can be adapted. Accordingly, the application of optimization techniques to the forming process of a particular metal requires a large expertise. However, most professionals in the process of forming lack this expertise, which is an obstacle to fully exploit the potential of forming process optimization. To overcome this obstacle, it is necessary for an optimization strategy, in forming process to adopt a structured approach that can solve major problems of metal forming. The subsequent sections are devoted to describe the optimization approach used in this work to enhance the metal forming process defined in previous sections. In the following scheme we are describing the different steps of resolution adopted in this work.

8.2. Optimisation methods in forming process

There are several methods to optimize forming processes such as: Newton method, genetic algorithms, design of experiments and Tagauchy techniques. These methods are used directly to deal with problems mathematically modelled based on mechanical models, or indirectly by example in learning sequences through artificial neural networks.

Classic method

Principle

The minimization of a function called cost function or objective function is the most used for the optimization of forming process. This function depends on several parameters that affect the calculation of first and second derivatives of the function. The number of function parameters to minimize also affects the number of iterations to obtain a solution that solves the whole problem [16].

Among the conventional common methods using the gradient of the function we are explaining briefly in the following paragraph the principle of this technique.

Considering f(x) the cost function to be minimized and Δf the gradient of this function. The algorithm will therefore seek to construct a sequence of points x_1 x_2 ... x_k x_3, such as indicated by [16]:

$$f(x_k+1) < f(x_k)$$

The algorithm therefore consists in the following expression:

$$x_k+1 = x_k - \alpha\, k\Delta f(x_k)$$

with α, the step taken in the direction of the highest slope. The stopping criterion may include a tolerance on the variation of the cost function, a tolerance on the variation of x, a tolerance value of the gradient, a maximum number of iterations or a maximum number of evaluations.

The effectiveness of this method is low. It can be shown that two consecutive directions will be orthogonal and that this feature may cause oscillations and lead to the divergence of the algorithm.

Choice of used method

According to previous sections, it was concluded that by taking some basic precautions into account, we are able to finally reproduce fairly well with a finite element simulation a forming process operation. thinning phenomenon is one of the most difficult to control during the development of stamping operations, because many parameters such as the geometry of tools, stamping speed, lubrication tools and so influence the geometry and residual stress state of the final product. This methodology is devoted primarily to the geometric configuration of the forming equipment and determining target parameters during optimization. The parameters are chosen to optimize the rays of the die and the punch as those factors are most sensitive in the forming process.

In general for a problem of single-objective optimization, we define an objective function (response function), we seek to optimize with respect to involved parameters. The objective function chosen in our case is the difference between the reference curve of the initial thickness of the plate and thickening of the curve obtained after numerical simulation via Abaqus explicit, this function is called monobjective function.

Let f(x) the objective function described as:

$$f(x) = e - y(x)$$

with: e – initial thickness of the blank; y(x) – thickness function, x – x coordination along the diagonal path.

We have applied optimization of mild steel deep drawing process, with initial blank thickness of 1.2 mm.

Looking for the thickening function

In the previous chapter, the FE numerical simulation using Abaqus software has allowed us to extract the thickening curves for different cases. However, it was not possible to extract the equations for these curves via Abaqus software. For this reason, we have chosen to use a mathematical curve fitting program included in Matlab software to provide an approximate equation of the curve thickening.
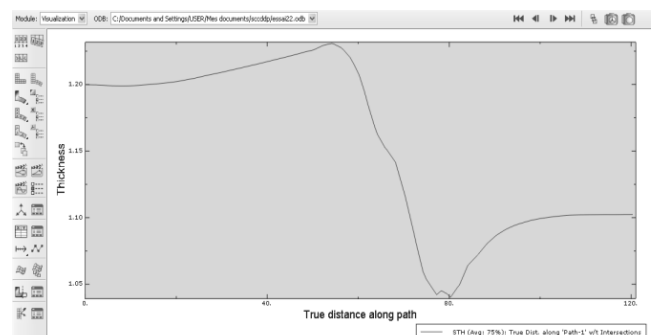
Fig. 38. Thickening vs. x distance along the diagonal path

Example: Here above is a thickening curve shown in Figure 38 obtained with: r_{sD}=0.25; r_{fP}=0.1; t_b=1.2 and l_D=1.

To know the equation describing this curve we extracted first the coordinate values of points forming the curve.

The values are then saved in a text file. After finishing with the numerical simulation by Abaqus, then data are imported to the Matlab workspace for example. Coordinate values of the thickness curve as shown in Figure 39.
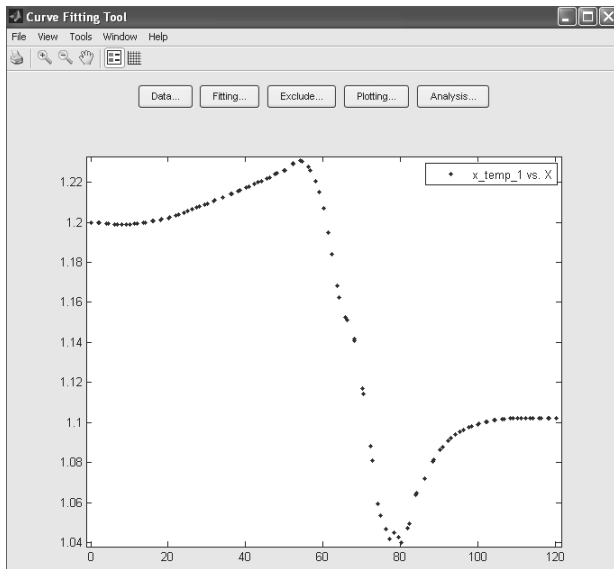
Fig. 39. Thickness distributions via Matlab software

The curve presented by Figure 39 is built from the coordinates of the thickness distribution extracted at first from FE results.

Indeed, in the next step we will choose the most suitable equation that overlies the shape of the curve formed by point list previously defined among all equations proposed by Matlab.
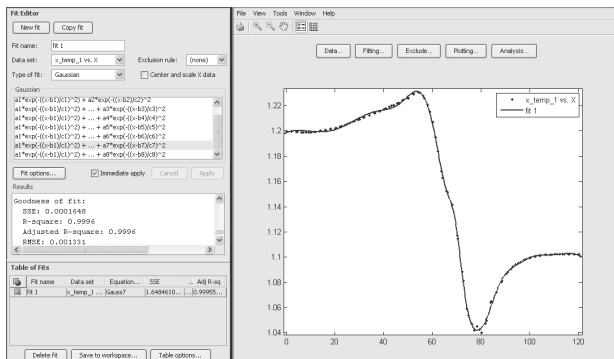
Fig. 40. Fitting results and statistics parameters

To verify the correct choice of the equation, there are statistical parameters that help us to take the right decision. These sets are listed in the fitting results window (Figure 40). They are represented as follows [16-18]:

- SSE (Sum of Square due to Error) is the sum of squared errors of adjustment. A value closer to zero indicates a successful adjustment;

- R-square: the square of the correlation between input values and predicted values after adjustment. A value closer to 1 indicates a good correlation between the actual and fitted values;

- adjusted R-square: it is the degree of freedom of R-square. A value closer to 1 indicates a better fit;

- RMSE: the root of the mean errors. A value closer to 0 indicates a good fit with less error.

Because our goal is to study the rate of thinning in a formed blank, we choose the values of thickness variations which are less than the initial thickness of the blank (1.2 mm). Indeed, areas at the final product whose thickness exceeds the value of the initial thickness of the blank, and undergo high thickening.

Then, we obtained for these values of thickness, the curve shown by Figure 41. In this case, the corresponding equation proposed by Matlab is an order 7 Gaussian curve with corresponding coefficients: Adjusted R-square and ESS are respectively closer to 1 and 0.
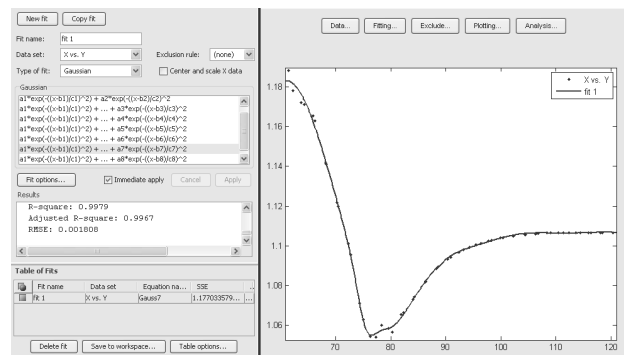
Fig. 41. Thinning curve

The best equation corresponding to the represented curve is as follows:

$$y(x)=a1*\exp(-((x-b1)/c1)^2) + ... + a7*\exp(-((x-b7)/c7)^2$$

Below are presented the equation coefficients with a confidence equal to 95%.
a1=0.4232 (-3.359, 4.206); b1=56.95 (26.06, 87.85); c1=19.18 (-58.1, 96.47)
a2=1.105 (1.067, 1.144); b2 = 122 (77.07, 167); c2=103 (-501.1, 707.2)
a3=0.04211 (-0.7084, 0.7926); b3=97.21 (22.51, 171.9); c3=12.88 (-57.95, 83.71)
a4=0.04122 (-0.3036, 0.386); b4=87.12 (74.04, 100.2); c4=8.848 (-10.05, 27.75)
a5=-0.0006871 (-0.06063, 0.05926); b5=88.92 (16.41, 161.4); c5=0.6008 (-47.75, 48.96)
a6=-0.01663 (-0.06769, 0.03444); b6=75.42 (74.6, 76.24); c6=2.121 (-0.2897, 4.532)
a7=-0.006177 (-0.06756, 0.05521); b7=78.68 (58.73, 98.64); c7=3.954 (-23.07, 30.98)

The best fit of this curve is obtained with the following equation

$$y(x)=a1*\exp(-((x-b1)/c1)^2) + ... + a7*\exp(-((x-b7)/c7)^2$$

Below are giving the equation coefficients with a confidence equal to 95%.
a1=0.4232 (-3.359, 4.206); b1=56.95 (26.06, 87.85); c1=19.18 (-58.1, 96.47)
a2=1.105 (1.067, 1.144); b2=122 (77.07, 167); c2=103 (-501.1, 707.2)

a3=0.04211 (-0.7084, 0.7926); b3=97.21 (22.51, 171.9); c3=12.88 (-57.95, 83.71)

a4=0.04122 (-0.3036, 0.386); b4=87.12 (74.04, 100.2); c4=8.848 (-10.05, 27.75)

a5=-0.0006871 (-0.06063, 0.05926); b5=88.92 (16.41, 161.4); c5=0.6008 (-47.75, 48.96)

a6=-0.01663 (-0.06769, 0.03444); b6=75.42 (74.6, 76.24); c6=2.121 (-0.2897, 4.532)

a7=-0.006177 (-0.06756, 0.05521); b7=78.68 (58.73, 98.64); c7=3.954 (-23.07, 30.98)

Optimization function

After determining the equation of the thickness curve, the objective function becomes equal to

$$f(x)=1.2-a1*exp(-((x-b1)/c1)\wedge2) + ... + a7*exp(-((x-b7)/c7)\wedge2$$

To optimize this objective function, we have used the function "fminbnd" performed in Matlab optimization toolbox which allows the minimization of a function in one variable in a fixed interval. The minimization function is then saved as an M-file and it is done with the following variables:
x=fminbnd (@(x) Abaqus (x,a1,b1,c1, a2,b2,c2, a3,b3,c3,a4,b4,c4, a5,b5,c5, a6,b6,c6 ,a7,b7,c7), 61.3441,120)
when we calculate the value of this minimized function we find:
f=0.0938 is thus obtained for x=107.1561 mm, f (x)=0.0938

The value found for f (x) becomes minimal. Otherwise for a distance 107.1561 mm we have less thinning.

By following the same steps as in the previous example, we calculate the functions minimized for different values of geometric parameters r_{sD}, R_{fP} and R_{sP}, R_{fD}. By comparing the values of f(x) obtained for different cases, we choose the lowest. Indeed, the objective function is minimal in our case a low rate of thinning. Therefore, the risk of occurrence of these defects decreases for selected parameters. It then derives the optimal values of these geometric parameters: radii of punch and die.

9. Search of optimal geometric parameters

9.1. Search of the optimal R_{sD} and r_{fP} values

Taking into account the previous example, we'll continue to look for other values and R_{sD} r_{fP} equations of thickness and objective functions to determine the optimal values of these parameters.
        r_{sD}=0.4 and r_{fP}=0.1
by adopting a similar methodology as in the previous example, we have determined the thickness equation as follows.

$$y(x)=a1*exp (-((x-b1)/c1)\wedge2) + ... + a6*exp (-((x-b6)/c6)\wedge2$$

with the following coefficients verifying a confidence value of 95%:
a1=0.1233 (-0.96, 1.207); b1=47.88 (-119.8, 215.6); c1=23.35 (-114, 160.7)
a2=1.102 (1.092, 1.113); b2=111.1 (-76.69, 298.9); c2=409.2 (-4854, 5672)
a3=-0.01318(-0.02148, -0.004891); b3=80.97 (80.73, 81.21); c3=1.791(0.9269, 2.656)

a4=-0.04269 (-0.3768, 0.2914); b4=81.04 (65.63, 96.45); c4=7.37(-16.51, 31.25)
a5=-0.04958 (-0.2447, 0.1455); b5=75.1 (72.75, 77.45); c5=4.8 (1.245, 8.356)
a6=-0.00895 (-0.1945, 0.1766); b6=89.27 (-74.38, 252.9); c6=10.83 (-96.06, 117.7)
with the following statistics parameters:
- SSE: 3.76exp5
- R-square: 0.9992
- Adjusted R-square: 0.9989
- RMSE: 0.001008

f(x) is minimal for x=113.5970 and its value is equal to:

$$f(x)=1.2-   y(x)   =a1*exp(-((x-b1)/c1)\wedge2)   +   ...   + a6*exp(-((x-b6)/c6)\wedge2 = 0.0972.$$

        r_{sD}=0.25 and r_{fP}=0.4:
The expression of the equation of thickness curve is done by:

$$y(x) = a1*exp(-((x-b1)/c1)\wedge2) + ... + a8*exp(-((x-b8)/c8)\wedge2$$

with the following equation coefficients verifying a confidence interval of 95%:
a1=0.08261 (0.002547, 0.1627); b1=59.03 (57.8, 60.26); c1=9.908 (7.012, 12.8)
a2=0.2163 (-1.124, 1.557); b2=49.75 (25.33, 74.17); c2=27.33 (-24.02, 78.69)
a3=1.181 (1.006, 1.356); b3=-2.879 (-37.2, 31.44); c3=83.14 (-143, 309.2)
a4=1.011 (-0.4632, 2.484); b4=127.5 (59.19, 195.7); c4 = 59.7 (22.14, 97.26)
a5=0.02191(-6.857*10^{13},6.857*10^{13});
b5=92.17(-5.312*10^{14}, 5.312*10^{14});
c5=0.1333(-3.626*10^{14}, 3.626*10^{14})
a6=0.04702 (0.03598, 0.05806); b6=69.88 (69.45, 70.31); c6=4.827 (4.127, 5.526)
a7=0.03335 (-0.02731, 0.09401); b7=85.62 (84.82, 86.42); c7=1.104 (-0.1832, 2.391)
a8=0.05877 (-0.1257, 0.2432); b8=93.79 (90.54, 97.05); c8=13.04 (2.518, 23.56)
and with the following statistics parameters:
- SSE: 6.083 exp (-5)
- R-square: 0.9988
- Adjusted R-square: 0.9978
- RMSE: 0.001424

f(x) is minimum for x=116.6013 mm and its value in this case is equal to:

$$f(x)=1.2-   y(x)   =a1*exp   (-((x-b1)/c1)\wedge2)   +   ...   + a8*exp(-((x-b8)/c8)\wedge2 = 0.0701$$

        r_{sD}=0.4 and r_{fP}=0.4
The expression of the equation of thickness curve is done by:

$$y(x) = a1*exp(-((x-b1)/c1)\wedge2) + ... + a8*exp(-((x-b8)/c8)\wedge2$$

with the following equation coefficients verifying a confidence interval of 95%:
a1=0.2897 (-0.9158, 1.495); b1=65.51 (57.54, 73.48); c1=9.022 (-4.807, 22.85)
a2=1.123 (1.091, 1.154); b2=121.5 (89.44, 153.6); c2=109 (-161.5, 379.5)

a3=0.04296 (0.03036, 0.05557); b3=85.75 (85.45, 86.04); c3=1.51(0.7563, 2.263)

a4=0.008928 (0.003119, 0.01474); b4=92.54 (92.04, 93.04); c4=1.22(0.1885, 2.251)

a5=0.002508 (-0.002666, 0.007682); b5=95.7 (93.4, 98); c5=2.061 (-1.371, 5.493)

a6=0.02983 (-0.03026, 0.08993); b6=80.13 (78.93, 81.33); c6=3.19 (0.268, 6.113)

a7=0.05673 (-0.5539, 0.6673); b7=90.55 (33.45, 147.6); c7=16.27 (-37.41, 69.95)

a8=0.01087 (-0.006902, 0.02865); b8=76.48 (75.28, 77.67); c8=1.868 (0.5105, 3.225)

The statistics parameters:
- SSE: 3.68 exp (-5)
- R-square: 0.9992
- Adjusted R-square: 0.9985
- RMSE: 0.001127

f (x) is minimum for x=117.6832 mm and its value is done by:

f(x)=1.2- y(x) = a1*exp(-((x-b1)/c1)^2) + ... + a8*exp(-((x-b8)/c8)^2 = 0.0749

$$r_{sD}=0.25 \text{ and } r_{fP}=0.2$$

The expression of the thickness curve in this case is done by:

y(x)=a1*exp(-((x-b1)/c1)^2) + ... + a8*exp(-((x-b8)/c8)^2

with the following coefficients verifying a confidence interval of 95%:

a1=0.184 (-9.013, 9.381); b1=65.78 (-249.3, 380.9); c1=10.08 (-127.5, 147.6)

a2=1.109 (1.109, 1.11); b2=112.5 (110.7, 114.2); c2=174.7 (84.74, 264.7)

a3=0.01317 (-0.1128, 0.1392); b3=87.55 (85.46, 89.64); c3=2.182 (-3.562, 7.926)

a4=0.05056 (-0.8239, 0.9251); b4=78.72 (72.03, 85.4); c4=3.801 (-13.13, 20.74)

a5=-0.1224 (-9.81, 9.565); b5=75.22 (-335.7, 486.1); c5=9.535 (-174.1, 193.2)

a6=0.04234 (-0.2425, 0.3272); b6=72.55 (70.14, 74.96); c6=2.922 (-0.5512, 6.396)

a7=0.005245 (-0.1151, 0.1256); b7=91.09 (80.96, 101.2); c7=2.504 (-10.01, 15.02)

a8=0.002789 (-0.06102, 0.0666); b8=96.13 (42.23, 150); c8=4.521 (-27.41, 36.46)

The statistics parameters are:
- SSE: 2.636exp-005
- R-square: 0.9996
- Adjusted R-square: 0.9993
- RMSE: 0.0009373

f(x) is minimal for x=112.5001 mm and its value in this case is done by:

f(x)=1.2- y(x) =a1*exp(-((x-b1)/c1)^2) + ... + a8*exp(-((x-b8)/c8)^2 = 0.0910

$$r_{sD}=0.2 \text{ and } r_{fP}=0.1$$

The equation of thickness curve is done by:

y(x) = a1*exp(-((x-b1)/c1)^2) + ... + a8*exp(-((x-b8)/c8)^2

with the following coefficients corresponding to a confidence interval of 95%:

a1=3.561exp5 (-1.926exp10, 1.926exp10); b1=-23.88 (-3.246exp5, 3.245exp5)

c1=21.45 (-4.56exp4, 4.565exp4); a2=1.306 (-8.893exp4, 8.893exp4)

b2=223.6 (-2.548exp7, 2.548exp7); c2=330.5 (-1.509exp7, 1.509exp7)

a3=-0.01705 (-0.02054, -0.01356); b3=75.5 (75.38, 75.63); c3=1.28 (0.9817, 1.578)

a4=0.02843 (-52.13, 52.18); b4=107.2 (-2887, 3101); c4=17.34 (-6722, 6756)

a5=0.145 (-45.07, 45.36); b5=64.37 (-703.4, 832.1); c5=10.47 (-523, 543.9)

a6=0.01094 (-0.009594, 0.03148); b6=86.76 (85.79, 87.73); c6=3.395 (1.021, 5.768)

a7=0.02533 (-1.735, 1.785); b7=92.57 (42.49, 142.7); c7=9.187 (-103.8, 122.2)

a8=-0.1288 (-5.514exp4, 5.514exp4); b8=167.3 (-1.126exp7, 1.127exp7)

c8=84.72 (-1.043exp7, 1.043exp7)

The statistics parameters are:
- SSE: 0.0001832
- R-square: 0.9982
- Adjusted R-square: 0.9978
- RMSE: 0.001427

f (x) is minimal for x=113.0403 and its value in this case is equal to:

f(x)=1.2- y(x) =a1*exp(-((x-b1)/c1)^2) + ... + a8*exp(-((x-b8)/c8)^2 = 0.0922

The previous results for the objective minimized functions f(x) are resumed in the following comparative Table 2.

Table 2.
Comparison between values of optimization functions

r_{sD}	0.25	0.4	0.25	0.4	0.25	0.2
r_{fP}	0.1	0.1	0.4	0.4	0.2	0.1
f(x)	0.0938	0.0972	0.0701	0.0749	0.0910	0.0922

According to this table, it is shown that the lowest value of f(x) is equal to 0.0701 corresponding to R_{sD}=0.25 and R_{fp}=0.4. For these two values of the radii of die and punch there is less thinning and high risk of defect occurrence within the end of the forming process. We can say that to optimize the forming process for a predefined material, it is preferable to choose the following values of R_{sD} r_{fP}, to minimize the problems of thinning as follows

$$r_{sD}=0.25 \text{ and } r_{fP}=0.4$$

In conclusion, at this stage of optimization, mathematical modeling show a decrease in the rate of thinning during forming process for $r_{fP} > 0.1$ and $R_{sD} < 0.6$, according to initial geometric parameters considered in this problem.

9.2. Search of the optimal r_{sP} and r_{fD} values

$$r_{sP}=0.4 \text{ and } r_{fD}=0.25:$$

Following the same steps as it was defined in the previous section. We have looked for the equation of y(x), and it was defined as:

y(x)=a1*exp(-((x-b1)/c1)^2) + ... + a6*exp(-((x-b6)/c6)^2

with the following coefficients that are done with a confidence interval of 95%:

$a1$=0.5184 (-1.462, 2.499); $b1$=62.29 (54.02, 70.56); $c1$=10.08 (-3.152, 23.31)

$a2$=1.102 (1.021, 1.183); $b2$=120.4 (85.83, 155); $c2$=77 (-150.5, 304.5)

$a3$=0.1308 (-1.291, 1.553); $b3$=87.15 (32.2, 142.1); $c3$=17.65 (-38.06, 73.37)

$a4$=-0.0149 (-0.01998, -0.009813); $b4$=78.87 (78.72, 79.03); $c4$=1.698 (1.266, 2.131)

$a5$=0.02207 (-0.0006604, 0.0448); $b5$=88.25 (87.27, 89.23); $c5$=4.342 (2.762, 5.921)

$a6$=0.141 (-0.0693, 0.3514); $b6$=74.45 (72.48, 76.42); $c6$=6.463 (3.651, 9.275)

The statistics parameters are done by:
- SSE: 2.208e-005
- R-square: 0.9997
- Adjusted R-square: 0.9995
- RMSE: 0.0007832

The function $f(x)$ is minimized for x=116.1692 mm, this means that there was minimum thinning after the sheet forming at the distance x=116.1692 mm and at this distance:

$$f(x)=1.2- \quad y(x) \quad =a1*exp(-((x-b1)/c1)^2) \quad + \quad ... \quad + a6*exp(-((x-b6)/c6)^2 = 0.0928$$

r_{sP}=0.4 and r_{fD}=0.4:

The equation of thickness curve is done by:

$$y(x)=a1*exp(-((x-b1)/c1)^2) + ... + a7*exp(-((x-b7)/c7)^2$$

with the following coefficients that are done with a confidence interval of 95%:

$a1$=0.2302 (-2.65, 3.11); $b1$=62.05 (16.38, 107.7); $c1$=16.41 (-21.98, 54.79)

$a2$=0.467 (-7.568, 8.502); $b2$=45.89 (-13.71, 105.5); $c2$=30.61 (-136.9, 198.1)

$a3$=1.166 (0.1066, 2.226); $b3$=-8.196 (-136.6, 120.2); $c3$=62.93 (-418.4, 544.3)

$a4$=0.1311 (-1.149, 1.411); $b4$=75.2 (55.89, 94.5); $c4$=8.671 (-6.359, 23.7)

$a5$=1.098 (-0.06019, 2.257); $b5$=122 (52.14, 191.8); $c5$=50.6 (-245.7, 346.9)

$a6$=-1.61 (-3848, 3844); $b6$=90.09 (-12.66, 192.8); $c6$=6.076 (-131.1, 143.2)

$a7$=0.1149 (-2.247, 2.477); $b7$=97.72 (35.94, 159.5); $c7$=12.14 (-58.56, 82.84)

The statistics parameters are done by:
- SSE: 2.369e-005
- R-square: 0.9995
- Adjusted R-square: 0.9992
- RMSE: 0.0008472

The function $f(x)$ is minimized for x=115.00 mm

$$f(x)=1.2-a1*exp(-((x-b1)/c1)^2) + ... + a7*exp(-((x-b7)/c7)^2 = 0.0790$$

r_{sP}=0.4 and r_{fD}=0.6:

The equation of thickness curve is done by:

$$y(x)=a1*exp(-((x-b1)/c1)^2) + ... + a8*exp(-((x-b8)/c8)^2$$

with the following coefficients that are done with a confidence interval of 95%:

$a1$=0.2302 (-2.65, 3.11); $b1$=62.05 (16.38, 107.7); $c1$=16.41 (-21.98, 54.79)

$a2$=0.467 (-7.568, 8.502); $b2$=45.89 (-13.71, 105.5); $c2$=30.61 (-136.9, 198.1)

$a3$=1.166 (0.1066, 2.226); $b3$=-8.196 (-136.6, 120.2); $c3$=62.93 (-418.4, 544.3)

$a4$=0.1311 (-1.149, 1.411); $b4$=75.2 (55.89, 94.5); $c4$=8.671 (-6.359, 23.7)

$a5$=1.098 (-0.06019, 2.257); $b5$=122 (52.14, 191.8); $c5$=50.6 (-245.7, 346.9)

$a6$=-1.61 (-3848, 3844); $b6$=90.09 (-12.66, 192.8); $c6$=6.076 (-131.1, 143.2)

$a7$=0.1149 (-2.247, 2.477); $b7$=97.72 (35.94, 159.5); $c7$=12.14 (-58.56, 82.84)

$a8$=1.721 (-3844, 3847); $b8$=90 (-25.39, 205.4); $c8$=6.195 (-132.3, 144.7)

The statistics parameters are done by:
- SSE: 6.142 exp(-5)
- R-square: 0.998
- Adjusted R-square: 0.9965
- RMSE: 0.001408

The function $f(x)$ is minimized for x=114.5862 mm and $f(x)$ is done with:

$$f(x)=1.2- \quad y(x) \quad =1.2-a1*exp(-((x-b1)/c1)^2) \quad + \quad ... \quad + a8*exp(-((x-b8)/c8)^2=0.0608$$

r_{sP}=0.4 and r_{fD}=0.8:

The equation of thickness curve is done by:

$$y(x)=a1*exp(-((x-b1)/c1)^2) + ... + a8*exp(-((x-b8)/c8)^2$$

with the following coefficients that are done with a confidence interval of 95%:

$a1$=0.08399 (-0.1323, 0.3002); $b1$=54.02 (36.61, 71.43); $c1$=24.35 (6.695, 42.01)

$a2$=1.198 (1.193, 1.204); $b2$=1.391 (-7.908, 10.69); $c2$=214.9 (-122, 551.8)

$a3$=0.2938 (-0.674, 1.262); $b3$=129.9 (111.4, 148.4); $c3$=33.79 (-23.17, 90.76)

$a4$=0.01307 (-0.008136, 0.03427); $b4$=75.81 (61.58, 90.04); $c4$=6.714 (-2.881, 16.31)

$a5$=-0.03196 (-0.06004, -0.00388); $b5$=80.54 (80.02, 81.06); $c5$=3.92 (2.943, 4.897)

$a6$=0.05901 (-0.2239, 0.3419); $b6$=93 (85.41, 100.6); $c6$=17.5 (-3.022, 38.02)

$a7$=0.006954 (-0.01532, 0.02923); $b7$=67.47 (58.15, 76.79); $c7$=5.481 (-0.4445, 11.41)

$a8$=0.04047 (-0.7717, 0.8526); $b8$=72.65 (69.85, 75.45); $c8$=6.073 (-23.08, 35.23)

The statistics parameters are done by:
- SSE: 1.541e-005
- R-square: 0.9991
- Adjusted R-square: 0.9985
- RMSE: 0.0006732

The function $f(x)$ is minimized for x=114.6336 mm, with $f(x)$ is done by the following

$$f(x)=1.2- \quad y(x) \quad =1.2-a1*exp(-((x-b1)/c1)^2) \quad + \quad ... \quad + a8*exp(-((x-b8)/c8)^2=0.0395$$

r_{sP}=0.25 and r_{fD}=0.25:
The equation of thickness curve is done by:

$$y(x)=a1*exp(-((x-b1)/c1)^2) + ... + a7*exp(-((x-b7)/c7)^2$$

with the following coefficients that are done with a confidence interval of 95%:
a1=0.1444 (-0.05489, 0.3437); b1=59.18 (56.11, 62.25); c1=11.05 (7.398, 14.71)
a2=0.2571 (-1.065, 1.579); b2=48.42 (23.3, 73.54); c2=24.93 (-14.48, 64.34)
a3=1.19 (1.096, 1.285); b3=0.05335 (-27.16, 27.27); c3=82.72 (-111.5, 277)
a4=0.9655 (-0.4893, 2.42); b4=124.1 (89.38, 158.7); c4=46.87 (-14.58, 108.3)
a5=0.09067 (0.03569, 0.1457); b5=70.36 (69.59, 71.13); c5=6.174 (5.017, 7.33)
a6=0.1376 (-0.4407, 0.7159); b6=89.13 (80.58, 97.68); c6=15.42 (-2.594, 33.44)
a7=0.02248 (0.01368, 0.03129); b7=79.17 (78.78, 79.55); c7=2.233 (1.411, 3.055)

The statistics parameters are done by:
- SSE: 2.685 exp (-5)
- R-square: 0.9996
- Adjusted R-square: 0.9993
- RMSE: 0.0008887

The function f(x) is minimized for x=116.6566 mm with f(x) is done by the following

f(x)=1.2- y(x) =1.2-a1*exp(-((x-b1)/c1)^2) + ... + a7*exp(-((x-b7)/c7)^2=0.0905

r_{sP}=0.6 and r_{fD}=0.25:
The equation of thickness curve is done by:

$$y(x) =a1*exp(-((x-b1)/c1)^2) + ... + a7*exp(-((x-b7)/c7)^2$$

with the following coefficients that are done with a confidence interval of 95%:
a1 = 0.155 (-0.9685, 1.279); b1 = 58.28 (55.85, 60.7); c1 = 10.51 (2.373, 18.65)
a2 = 0.8499 (-1.344, 3.044); b2 = 40.92 (-14.37, 96.2); c2 = 26.09 (-141, 193.2)
a3 = 1.096 (0.06832, 2.124); b3 = -6.846 (-41.14, 27.45); c3 =28.57 (-166.7, 223.8)
a4 = 0.2629 (-2.187, 2.713); b4 = 74.28 (57.65, 90.9); c4 =12.88 (-11.7, 37.45)
a5 = 1.104 (1.085, 1.123); b5 =117.3 (106.8, 127.8); c5 = 63.62 (-54.77, 182)
a6 = 0.04622 (-0.03824, 0.1307); b6 = 90.81 (89.95, 91.66); c6 = 5.024 (2.523, 7.525)
a7 =0.07014 (-0.2923, 0.4326); b7 = 97.29 (84.34, 110.2); c7 = 9.485 (-7.38, 26.35)

The statistics parameters are done by:
- SSE: 5.271e-005
- R-square: 0.999
- Adjusted R-square: 0.9985
- RMSE: 0.001264

The function f(x) is minimized for x=111.2032 mm, with f(x) is done by the following

f(x)=1.2- y(x) =1.2-a1*exp(-((x-b1)/c1)^2) + ... + a7*exp(-((x-b7)/c7)^2=0.0950

for the different cases considered in this section, we will extract optimal values of r_{sP} and r_{fD} parameters according to the comparative values in the Table 3 below.

Table 3.
Comparison of optimization results

r_{sP}	0.4	0.4	0.4	0.4	0.25	0.6
r_{fD}	0.25	0.4	0.6	0.8	0.25	0.25
F(x)	0.0928	0.0790	0.0608	0.0395	0.0905	0.0950

Comparing the results presented in the table, we notice that f(x) is minimal for $r_{sP}=R_{fD}$=0.4 and 0.8. We can conclude then the following optimal values:

$$r_{sP}=R_{fD}=0.4 \text{ and } 0.8$$

We checked in the previous chapter for a square plate with thin $r_{sP} < R_{fD}$ (more precisely $r_{sP}=R_{fD}$=0.4 and 0.6) there is less risk of developing thinning process during formatting. Therefore, with the optimal values of R_{sP} and R_{fD}, you get a quality product.

10. Conclusions

In order to improve the comprehension of some experimental results that we may face in the industrial deep drawing process, a larger parametric analysis is needed. Analysis using FEM parametric study is therefore indispensable. Nevertheless, a best FEM model has to be at the same time the lower in the CPU cost time and closely the most representative to experimental cases.

In this study we have conceived a FEM model of parametric deep drawing process analysis, a spectrum consisting of 136 geometries is used to assess a sheet metal DDP. As a first step, the numerical simulation using dynamic explicit finite element analysis has been validated within existing experimental data. This validation has concerned (MS material), different punch travels, various blank thicknesses; a good correlation has been noticed between experimental and simulated results.

The second step which is the major objective of this study consists on a geometric parametric FEA study. In fact, even though we have a large amount of numerical investigations in the literature review through this last decade; a specific detailed parametric study that involves the most dominating deep drawing parameters is well suitable at this stage. To emphasize interaction between the most fluctuant of this parameters we have choose to deal with the following.

In this paper, effect of the following geometric parameters (r_{sP}, r_{fD}, r_{fP}, r_{sD}, l_D, s_P and t_b) and their interaction on drawability of DDP are well analyzed. In particular, their sensitivity to thinning phenomena and thickness distribution along critical paths were obtained according to this trail;

As it is known the increase of r_{sD} parameter leads to diminishing of the maximum thinning in general, but it was observed that a law value of the fillet punch radius associated with a high blank thickness leads to a growth of maximum thinning and sometimes to wrinkling. In addition, the larger the aspect ratio l_D is, the smaller the maximum thinning particularly for deep drawing punch travels. These results could be effectively applied to produce successful DDP.

Once the numerical simulations have grasp the most important parameters effect on the DDP of a general rectangular cup, we have designed a statistical scheme to represent clearly and quantitatively the influence of this parameter using the statistical tool box. This has lead to interesting interpretation of the data provided from numerical FE simulations within the Abaqus commercial code. This fact, can give much more interest and precision to describe the influence and the importance degree of each geometric variable. FE analysis associated to an optimization tool; mono-objective function has been described. This study could further improve the final quality of parts produced by adapting the optimization method to determine the optimal values of geometric parameters of the DDP tools.

Nomenclature

W_P: width of the punch section
W_B: width of the blank
W_D: width of the die cavity
tL_P: total length of the punch section (for rectangular cups)
tL_B: total length of the blank (for rectangular cups)
tL_D: total length of the die cavity (for rectangular cups)
R_{fD}: fillet radius of the die
R_{fP}: section radius of the punch
R_{sD}: section radius of the die
R_{sP}: section radius of the punch
t_b: initial thickness of the sheet metal blank
V_P: punch speed
S_P: punch travel (stroke)
σ_Y: yield stress
E: Young's modulus
l_D: die normalized aspect ratio; $l_D = tL_D / W_D$
l_B: blank normalized aspect ratio; $l_B = tL_B / W_B$
r_{sP}: section normalized radius of the punch
r_{sD}: section normalized radius of the die
r_{fD}: fillet normalized radius of the die
r_{fP}: fillet normalized radius of the punch
$_{SP}$: normalize punch travel (stroke)

References

[1] L. Duchêne, A.M. Habraken, Analysis of the sensitivity of FEM predictions to numerical parameters in deep drawing simulations, European Journal of Mechanics A/Solids 24/4 (2005) 614-629.

[2] F. Fereshteh-Saniee, M.H. Montazeran, A comparative estimation of the forming load in the deep drawing process, Journal of Materials Processing Technology 140/1-3 (2003) 555-561.

[3] M. Colgan, J. Monaghan, Deep drawing process: analysis and experiment, Journal of Materials Processing Technology 132/1-3 (2003) 35-41.

[4] Z.Y. Cai, M.Z. Li, Multipoint forming of three-dimensional sheet metal and the control of the forming process, International Journal of Pressure Vessels and Piping 79/4 (2002) 289-296.

[5] R. Padmanabhana, M.C. Oliveiraa, J.L. Alvesb, L.F. Menezesa, Influence of process parameters on the deep drawing of stainless steel, Finite Elements in Analysis and Design 43 (2007) 1062-1067.

[6] Abaqus/Explicit manuel, version 6.7, Dassault Systèmes, Providence, RI, 2007.

[7] E. Bayraktar, S. Altintas, Square cup deep drawing and 2D-draw bending analysis of Hadfield steel, Journal of Materials Processing Technology 60/1-4 (1996) 183-190.

[8] J. Wang, R.H. Wagoner, A Practical Large Strain Solid Finite element for sheet forming, International Journal for Numerical Methods in Engineering 63 (2005) 473-501.

[9] J.H. Lee, B.S. Chun, Investigation on the variation of deep drawability of STS304 using FEM simulations, Journal of Materials Processing Technology 159/3 (2005) 389-396.

[10] F.K. Chen, T.B. Huang, C.K. Chang, Deep drawing of square cups with magnesium alloy AZ31 sheets, International Journal of Machine Tools and Manufacture 43/15 (2003) 1553-1559.

[11] M.P. Miles, J.L. Siles, R.H. Wagoner, K. Narasimhan, A better sheet formability test, Metallurgical and Materials Transactions A 24 (1993) 1143-1151.

[12] N.A. Maslennikov, Russian developed punchless drawing, Metalwork Productions 16 (1957) 1417-1420.

[13] A.M. Prior, Applications of Implicit and explicit Finite Element Techniques to metal forming, Journal of Materials Processing Technology 45 (1994) 649-656.

[14] Y.T. Keum, R.H. Wagoner, J.K. Lee, Friction model for FEM simulation of sheet metal forming operations (N328), Proceedings of the 8th International Conference "Numerical Methods in Industrial Forming Processes" NUMIFORM 2004, Columbus, 2004, 989-994.

[15] E. Daxin, T. Mizunob, L. Zhiguo, Stress analysis of rectangular cup drawing, Journal of Materials Processing Technology 205/1-3 (2008) 469-476.

[16] J. F. Bonnans, J.Ch. Gilbert, C. Lemaréchal, C. Sagastizábal, Numerical optimization, theoretical and numerical aspects, Springer, 2006.

[17] M. Bierlaire, Introduction à l'optimisation différentiable, Presses-Polytechniques et Universitaires Romandes, 2006 (in French).

[18] Y.Q. Guo, J.L. Batoz, H. Naceur, S. Bouabdallah, F. Mercier, O. Barlet, Recent developments on the analysis and optimum design of sheet metal forming parts using a simplified inverse approach, Computers and Structures 78/1-3 (2000) 133-148.